

Glucose Responsive Hydrogels: Synthesis and Investigation of the Biomedical Applications

Mosab Abu Reesh

Submitted to the
Institute of Graduate Studies and Research
in partial fulfillment of the requirements for the degree of

Doctor of Philosophy
in
Chemistry

Eastern Mediterranean University
September 2015
Gazimağusa, North Cyprus

Approval of the Institute of Graduate Studies and Research

Prof. Dr. Serhan Çiftçiođlu
Acting Director

I certify that this thesis satisfies the requirements as a thesis for the degree of Doctor of Philosophy in Chemistry.

Prof. Dr. Mustafa Halilsoy
Chair, Department of Chemistry

We certify that we have read this thesis and that in our opinion it is fully adequate in scope and quality as a thesis for the degree of Doctor of Philosophy in Chemistry.

Assoc. Prof. Dr. Mustafa Gazi
Supervisor

Examining Committee

1. Prof. Dr. Ayfer Saraç

2. Prof. Dr. Bahire Filiz Őenkal

3. Prof. Dr. Elvan Yılmaz

4. Assoc. Prof. Mustafa Gazi

5. Asst. Prof. Dr. Hayrettin Ozan Gölcan

ABSTRACT

The growing rate of diabetes mellitus (DM) has called for urgent concern among researchers and expert in the field of drug delivery. Hence, the present work synthesized pH and glucose-sensitive hydrogels with promising antibacterial applications. The hydrogel (CS–PVA) was synthesized via boric acid crosslinking and freeze-thawing cycle techniques. The surface chemistry of CS–PVA hydrogel was confirmed by scanning electron microscopy and Fourier transform infrared spectroscopy.

The hydrogel displayed high glucose-sensitivity under physiological conditions, and its sensitivity was noticed to increase in the presence of varied glucose concentrations. Additionally, the swelling and drug loading behavior of the hydrogel was influenced by the pH of the medium. Under optimized conditions, the cumulative drug releases ranged between 33–86% for bovine serum albumin and 39–92% for insulin at 37°C in PBS solutions and in the presence of glucose. The synthesized hydrogel exhibited excellent antibacterial activity and was found to reduce the growth of *E.coli* (gram negative) bacterial by 86.5%.

Keywords: Chitosan; glucose sensitivity; drug delivery; antibacterial; hydrogels; swelling; optimization.

ÖZ

Diabetes mellitus'un (DM) büyüme hızı, ilaç taşınımı alanındaki uzman ve araştırmacılara acilen ihtiyaç çağrısında bulunmaktadır. Bu nedenle, bu çalışmada umut verici antibakteriyel uygulamalara sahip, pH ve glukoz-duyarlı hidrojeller sentezlenmiştir. Hidrojel (CS—PVA), çapraz bağlayıcı borik asit ve donma-çözülme döngüsü teknikleri ile sentezlenmiştir. CS—PVA hidrojelinin yüzey kimyası taramalı elektron mikroskobu ve Fourier kızılötesi spektroskopisi ile teyit edilmiştir.

Hidrojel fizyolojik koşullar altında, yüksek glukoz duyarlılığı göstermekte ve artan glukoz konsantrasyonları varlığındaki duyarlılığı gelişme göstermektedir. Ayrıca, hidrojel şişme ve ilaç yükleme davranışı ortamının pH etkilenmektedir. Optimum koşullar altında, kümülatif ilaç serbest salınım değerleri glukoz varlığında, bovin serum albümin için 37°C'de %33—86 ve PBS içinde çözeltiler de insülin için %39—92 aralığında değişmektedir. Sentezlenmiş hidrojel mükemmel bir antibakteriyel aktivite sergilemiş ve bakteriyel büyümede % 86,5 E.coli (gram negatif) azalmasına yol açtığı saptanmıştır.

Anahtar Kelimeler: Kitosan; glukoz duyarlılığı; ilaç taşınımı; antibakteriyel; hidrojel; şişme; optimizasyon.

DEDICATION

To my dear Palestine

The place that I left and I'll be back to serve for its land

To my honorable father - Abu Ahmad

To my lovely mother - Um Ahmad

To my brothers; Ahmad, Mohammad, Abdur-Rahman, Anas and Mujahid

To my sisters, uncles, aunts, cousins, grandmother, and all my relatives

To my beautiful wife Um Rayan

To my soul and my little baby Rayan

To all of them I would like to dedicate my efforts.

Best Regards,

Mosab Abu Reesh

ACKNOWLEDGMENT

I would like to thank my supervisor (Assoc. Prof. Dr. Mustafa Gazi) for his supervisory support and guidance during my PhD study. I must stress that his efforts and flexibility worth a lot to me, without which I could have been hampered.

I am immensely grateful to Dr. Akeem Adeyemi Oladipo for his understanding, patience, tolerance, assistance, support and also friendship.

I am also obliged to Asst. Prof. Dr. Imge Kunter for her help during my thesis. Besides, a number of friends had always been around to support me morally. I would like to thank them as well.

I owe quite a lot to my family who allowed me to travel all the way from Palestine to Cyprus and supported me all throughout my studies. I would like to dedicate this study to them as an indication of their significance in this study as well as in my life.

TABLE OF CONTENTS

ABSTRACT	iii
ÖZ	iv
DEDICATION	v
ACKNOWLEDGMENT	vi
LIST OF TABLES	ix
LIST OF FIGURES	x
LIST OF SCHEMES	xii
1 INTRODUCTION	1
1.1 Aim and Scope of Study	5
2 LITERATURE REVIEW.....	6
2.1 Smart Hydrogel Based Systems	6
2.1.1 Classification of Smart Hydrogels	8
2.1.1.1 pH-sensitive Hydrogels	
2.1.1.2 Glucose-sensitive Hydrogels	
2.2 Chitosan Based Hydrogel systems for different biomedical application.....	14
2.3 Drug Release Mechanism	17
2.4 Hydrogels as Antimicrobial Agents	19
3 EXPERIMENTAL	21
3.1 Chemicals and Materials	21
3.2 Synthesisof Boric acid cross-linked Chitosan/PVA hydrogel	21
3.3 Characterization	22
3.4 Swelling Studies.....	22
3.5 Drug Release Experiments and Optimization.....	22

3.6 CS–PVA Hydrogel Antibacterial Test.....	23
4 RESULT AND DISCUSSIONS	24
4.1 Synthesis and Characterization of Hydrogels	24
4.2 Swelling Properties of CS–PVA Hydrogels and pH Sensitivity	28
4.3 Glucose-sensitivity of CS–PVA Hydrogel	32
4.4 Swelling Behavior of the CS–PVA Hydrogel in Physiological Fluids	35
4.5 Experimental Design for Drug Loading Efficiency and Capacity	36
4.6 Drug Release Analysis, Optimization, and Mechanism	40
4.6.1 BSA Release.....	40
4.6.2 Insulin Release	42
4.6.3 Mechanism and Modeling of In <i>vitro</i> Release Kinetic of CS–PVA Hydrogel.....	45
4.7 Antimicrobial Activity of CS–PVA hydrogel	50
5 CONCLUSION	54
REFERENCES.....	55

LIST OF TABLES

Table 1. Experimental design layout for BSA loading and the obtained results	38
Table 2. ANOVA for response surface quadratic model for BSA loading onto CS-PVA.....	39
Table 3. Drug release kinetic parameters for CS-PVA in different release media ...	46
Table 4. Drug release kinetic parameters for CS-PVA in different release media ...	49

LIST OF FIGURES

Figure 1. Summary of the most remarkable symptoms of diabetes (Mikael	3
Figure 2. Schematic representation of the scope of this thesis	5
Figure 3. Structure of typical hydrogel (Mahdavinia et al., 2014).....	6
Figure 4. Smart or stimuli-responsive hydrogel.....	7
Figure 5. Summarized classification of smart hydrogels	8
Figure 6. Pictorial description of pH-dependent hydrogel system.....	9
Figure 7. Apictorial representation of pH-sensitive swelling of ionic hydrogels	10
Figure 8. Pictorial representation of glucose-sensitive hydrogels	11
Figure 9. Three main classes of glucose-sensitive hydrogels	12
Figure 10. Complex between a sugar molecule and PBA moiety in aqueous solution	13
Figure 11. Pictorial representation of drug release mechanism	18
Figure 12. Antibacterial mechanism of polymer composite	20
Figure 13. FTIR spectrum of CS, PVA and CS–PVA hydrogel.....	26
Figure 14. SEM image of CS–PVA hydrogel.....	27
Figure 15. SEM photographs of optimized BSA-loaded hydrogel	28
Figure 16. Swelling ratio of CS–PVA hydrogel in distilled water, acid, and basic...	29
Figure 17. Pseudo-Fickian plot for fractional uptake of water by CS–PVA hydrogel	31
Figure 18. Pseudo-Fickian plot for fractional uptake of acid solution by CS–PVA .	31
Figure 19. Pseudo-Fickian plot for uptake of basic solution by CS–PVA hydrogel .	32
Figure 20. Swelling behavior of CS–PVA hydrogel in PBS (pH 7.4) at various	33
Figure 21. Swelling ratio of the CS–PVA hydrogel in physiological fluids	35

Figure 22. Response surface of the combined effects of pH, time and.....	37
Figure 23. Cumulative release (CR) % of BSA from CS–PVA in different PBS pH	41
Figure 24. The stepwise response of CS–PVA hydrogels at fixed glucose.....	42
Figure 25. Cumulative release (CR) % of insulin from CS–PVA in different varied	43
Figure 26. Pareto chart for individual and interactive effects of factors affecting	44
Figure 27. (a) The total amount of BSA and (b) insulin release versus square root of	47
Figure 28. (a) The fraction of BSA released vs. time (b) insulin released vs. time ...	49
Figure 29. The photograph of the inhibition zones of CS–PVA hydrogel against ...	50
Figure 30. Effect of CS–PVA hydrogel on the growth of E.coli	51
Figure 31. Antibacterial test showing the efficacy of CS–PVA hydrogel against....	52

LIST OF SCHEMES

Scheme 1. Synthesis route for boric acid crosslinked CS–PVA hydrogel	24
Scheme 2. Picture of the synthesized CS–PVA hydrogel	25
Scheme 3. Mechanism of glucose complexation with CS–PVA hydrogel.....	34

Chapter 1

INTRODUCTION

Diabetes mellitus (DM) is a worldwide metabolic disease that presently accounts for 8% of the world's population. The health complications and risks associated with DM is one of the leading causes of disabilities (viz.; heart disease, blindness, stroke, ketoacidosis, kidney failure, etc.) and death (Orthner et al., 2010; Lin, 2010). DM is due to the fact that the control of body blood sugar is compromised (Figure 1), either because the pancreas fails to produce enough insulin (Type 1 DM), or cells are not responding properly to the insulin produced (Type 2 DM). So far, no cure has been reported for diabetes. However, the main path to reduce its risks is constant monitoring of patient's blood glucose level, and then therapeutic intercession. For long-term management of DM, explicit measurements of blood glucose levels are extremely important since blood glucose levels in patient's exhibit swings throughout the day (Bindra et al., 1991).

However, the present widely utilized devices (glucose meters and test strips) provide only discontinuous information and cannot account for sudden fluctuations of blood glucose level (Bindra et al., 1991; Lin, 2010). As reported by Lin (2010), **fingerstick method** is also a widely applied glucose sensing technique. Here, an electrochemical sensor is used to test glucose concentration of blood removed from the fingertip of diabetic patients. The fingerstick approach is quite painful, hence patient concession is poor. Also, the fingerstick technique evidently cannot be applied to monitor

glucose level when the patient is sleeping. Hence, the fingerstick approach is not acceptable for strict monitoring of blood sugar levels. Recently enzyme based sensors have been developed for continuous glucose monitoring, such as implantable electrochemical systems (MiniMed Paradigm, Freestyle Navigator, etc.). These enzyme-based sensors display high specificity to glucose detection. However, they are problematic in several ways such as (Gerlach et al., 2005; Richter et al., 2008; Steege et al., 2007; Trinh et al., 2006):

- a. The utilization of glucose-restrictive membranes
- b. The dependence on glucose diffusivity as well as the blood oxygen level
- c. The frequent calibrations requirement and constant signal drifts over time
- d. The instability of the enzyme
- e. Fouling under physiological conditions
- f. Infection and inflammation that result from breaching the skin with a needle.

For these limitations, enzyme-based glucose sensors have been approved majorly for professional use with a short lifetime (Richter et al., 2008). Therefore, the development of alternative enzyme-free glucose sensing systems is necessary, and thus exclusive attention has been geared toward the development of glucose-sensitive hydrogels (G-SHs). The G-SHs are cross-linked biopolymeric materials that can reversibly change their properties, shapes, or volumes in response to changes in glucose concentration (Lin, 2010 Wilson and Hu, 2000).

Thus, coupling a micron-scale thickness G-SH to a pressure or optical measurements system can result into effective and strict glucose detection sensor for diabetic patients (Lin, 2010). Also, pH is also an important parameter for diabetes (Lin, 2009).



Figure 1. Summary of the most remarkable symptoms of diabetes (Mikael Häggström)

Thus, the proposed G-SH must be sensitive to both pH and environmental glucose. The objective of this thesis is to develop smart, low-cost hydrogels for continuous monitoring of both pH and glucose. The fundamental principle of the proposed smart sensor is the change of osmotic swelling pressure in response to variations in solution pH and environmental glucose concentration. We believe that the biocompatible non-enzyme based sensor will outstrip some of the limitations of current glucose monitoring systems and provide better diabetes management scheme. Intensive research efforts have been committed to developing glucose-sensitive polymeric systems and insulin delivery technologies, due to rapidly increasing diabetic population (Mahdavinia et al., 2014; Nayak et al., 2013; Reddy et al., 2013). It is

particularly important to develop biocompatible glucose-responsive system. Until now, three major kinds of glucose-sensitive hydrogels have been reported including hydrogel containing phenyl boronic acid group, lectin-loaded and glucose-oxidase loaded (Gade et al. 2006; Wang et al., 2010; Zhang et al., 2006). However among these, the phenyl boronic acid (PBA) moiety is the ideal candidate for glucose sensor because it can overcome issues such as toxicity, stability and immunogenicity associated with latter types.

Hydrogels containing chitosan and polyvinyl alcohol (PVA) have been identified to be suitable for biomedical applications due to their biocompatibility, stability, antibacterial and non-toxic features (Oladipo and Gazi, 2014a). Boric acid is well known for its use as a home remedy due to its medicinal properties (Manna and Patil, 2009); however, less information has been reported on boric acid cross-linked chitosan-based hydrogels for glucose sensing. The presence of boric acid within the CS-PVA network can improve the stability of the resulting hydrogel, and the boric acid derivative can easily interact with diols, making it suitable for glucose sensing.

Hence, boric acid cross-linked CS-PVA hydrogels showing high swelling at neutral pH and low swelling at low pH value have been developed in this study. The synthesized hydrogels containing boric acid selectively and reversibly bind with glucose. This result in volume changes of the CS-PVA hydrogel system driven by variation in glucose concentration. The glucose-responsive behaviour occurred at physiological pH, and the drug release behaviour of insulin and bovine serum albumin (BSA) from the hydrogel were optimized using response surface methodology. The developed hydrogel is highly attractive in terms of glucose sensitivity, self-regulated drug delivery and possess antibacterial property.

1.1 Aim and Scope of Study

The present study focuses on the preparation of pH and glucose-sensitive hydrogels; the resulting hydrogels were characterized and applied for antibacterial functions.

Figure 2 shows the schematic scope of this thesis:

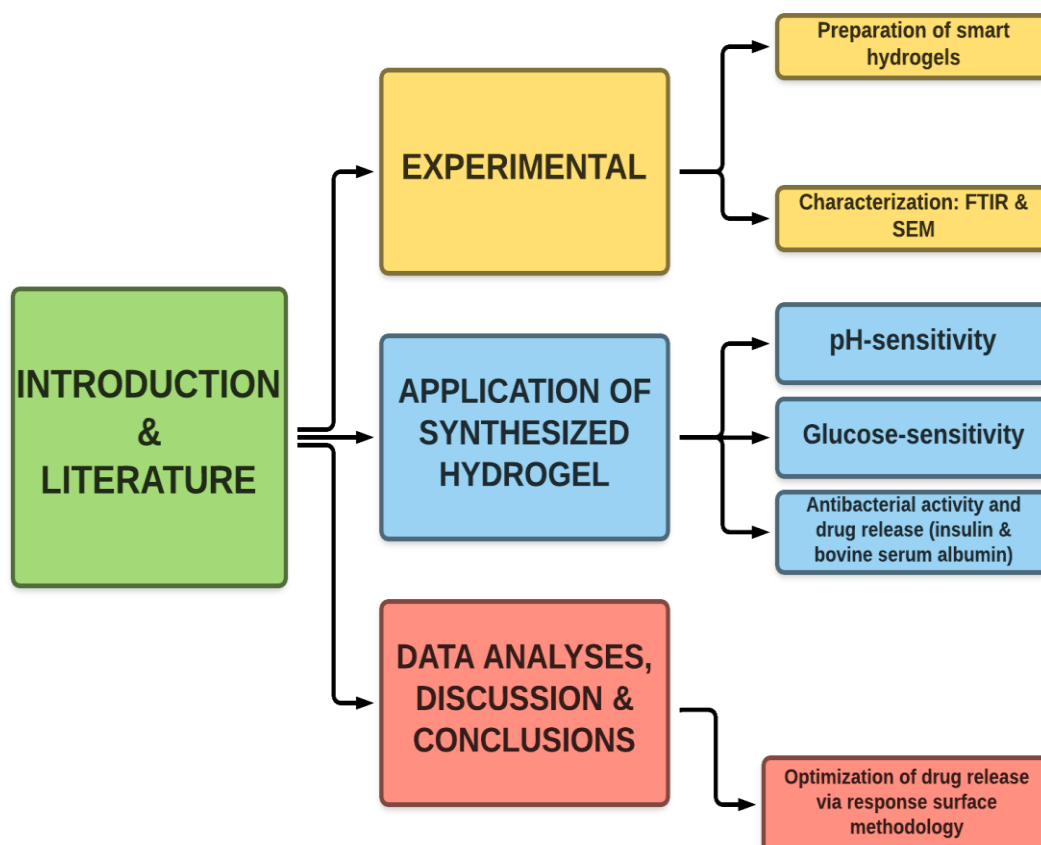


Figure 2. Schematic representation of the scope of this thesis

Chapter 2

LITERATURE REVIEW

2.1 Smart Hydrogel Based Systems

Hydrogels are cross-linked three-dimensional networks of hydrophilic polymer that can absorb a large quantity of fluid/water but do not dissolve in the medium. Hydrogels are versatile materials and can be tailor-made to specific requirements via manipulation of the processing and chemistry protocols. The three-dimensional structure of the hydrogels (Figure 3) in their swollen state are usually sustained either by the presence of chemical crosslinker or physical crosslinking points within the complex. Additionally, some functional groups ($-OH$, $-CONH_2$, $-CONH$, and $-COOH$) have been identified to enhance the hydrogel ability to absorb more fluid/water.

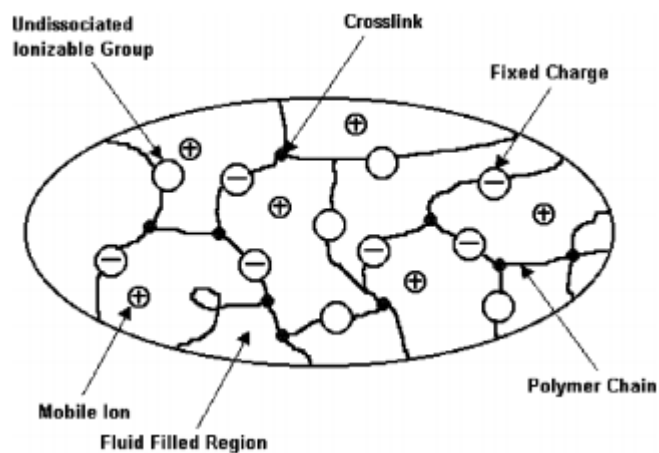


Figure 3. Structure of typical hydrogel (Mahdavinia et al., 2014)

‘Smart’ or ‘stimuli-responsive’ hydrogels (Figure 4) are cross-linked polymeric network that reversibly swells/shrinks in response to variations in external stimuli such as change in solution pH, ionic strength, system temperature, and concentration of some analyte (Nayak et al., 2013).

Smart hydrogels undergo changes in their physicochemical properties due to the presence of certain functional groups along the polymeric chains. These hydrogels have been utilized in diverse applications such as immobilization of enzymes, biological coatings, drug delivery system, artificial muscle, implantable biomedical sensors and gene delivery vectors. In this thesis, attention is paid comprehensively to glucose-sensitive and pH-sensitive hydrogels; however, other smart hydrogel systems are briefly presented.

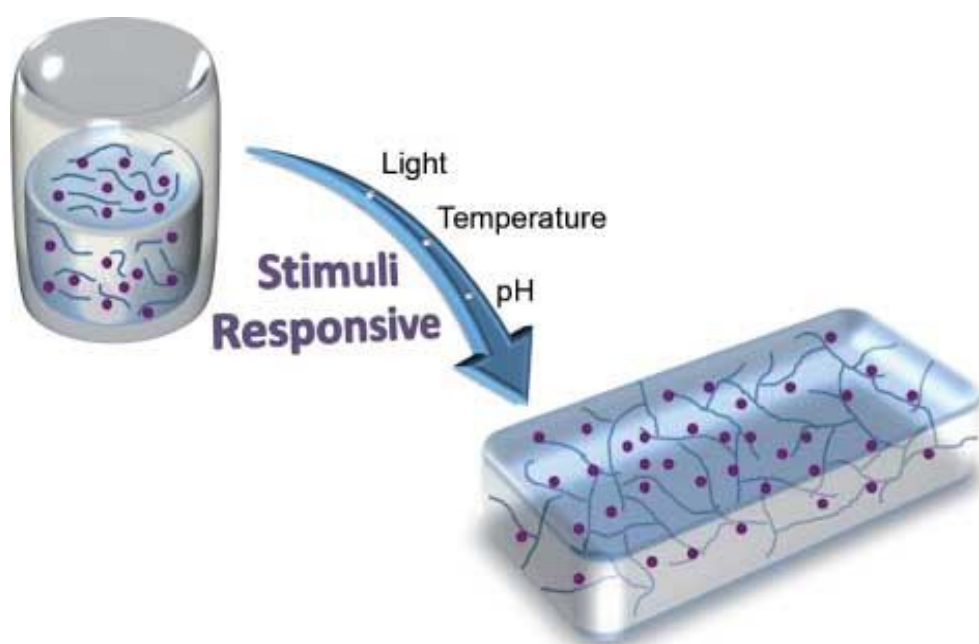


Figure 4. Smart or stimuli-responsive hydrogel

2.1.1 Classification of Smart Hydrogels

Smart hydrogels changed their network structure, swelling behavior, permeability, and mechanical strength in response to environmental changes. Sometimes these groups of hydrogels are called intelligent hydrogels or environmentally sensitive hydrogels. They can be classified into different groups based on the stimuli within the system; a summarized classification is presented in Figure 5:

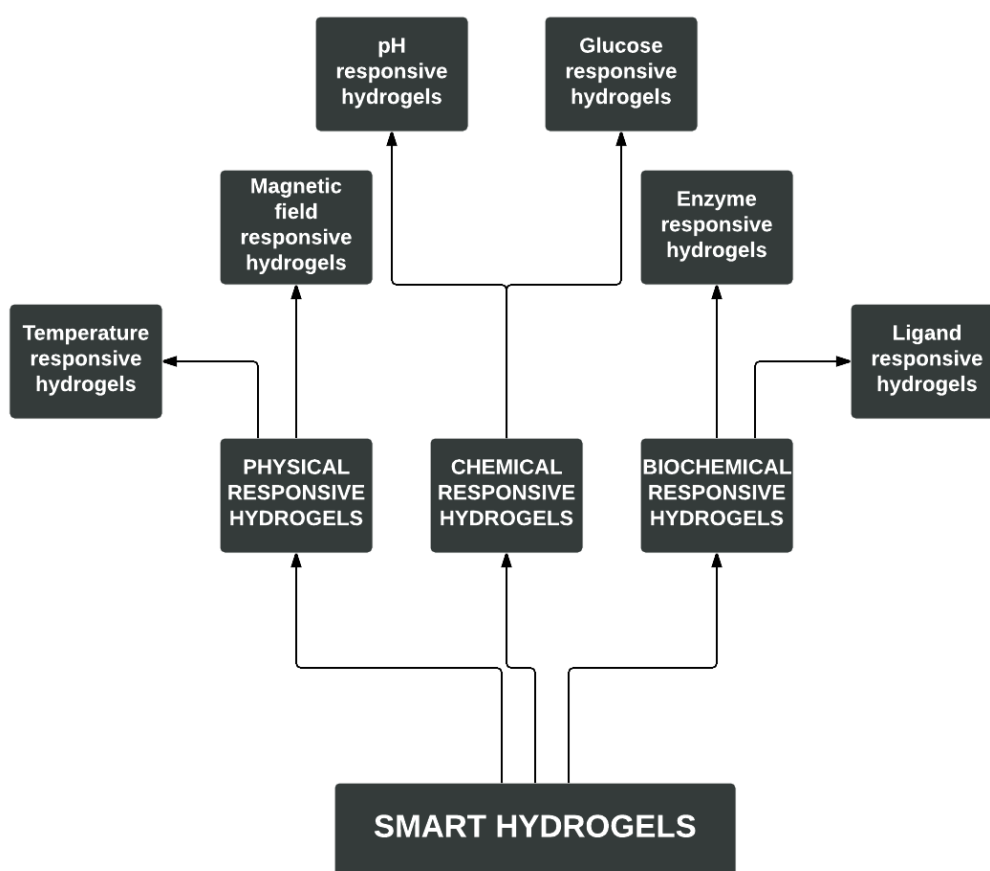


Figure 5. Summarized classification of smart hydrogels

The chemical stimuli-based hydrogels can change the interactions between polymer chains and a solvent or within the polymer chains in the presence of chemical agents. Similarly, physical factors such as mechanical stress, temperature, electric or magnetic fields can change the molecular interactions of polymer networks (Reddy et al., 2013).

2.1.1.1 pH-sensitive Hydrogels

The hydrogels that have the ability to accept or/and donate protons in response to pH variations are classified as pH-sensitive hydrogels (Figure 6). Changes in pH are known to take place at various body sites, including the vagina, blood vessels and gastrointestinal tract (Gupta et al., 2002), and these variations can proffer a suitable means for pH-sensitive drug release. Additionally, local pH variations in response to particular substrates can be obtained and utilized for modulating drug release. As reported by Gupta et al., (2002), pH-sensitive hydrogels are usually polymeric backbones containing ionic pendant groups including poly (acrylic acid), poly (dimethylaminoethyl methacrylate), poly (acrylamide) and poly (methacrylic).

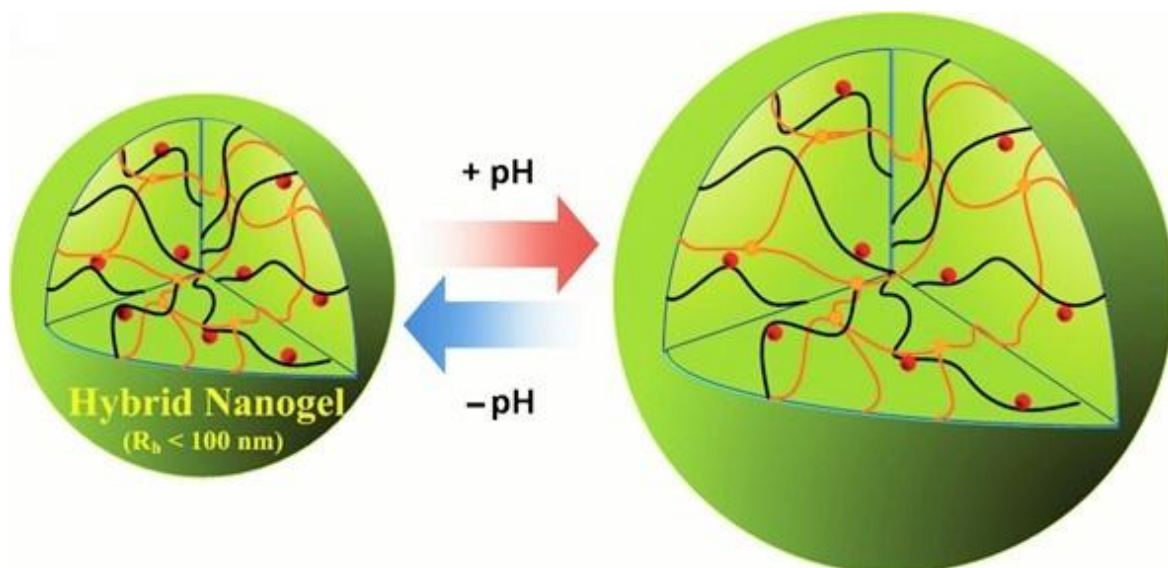


Figure 6. Pictorial description of pH-dependent hydrogel system

In aqueous environment of suitable ionic strength and pH, the smart hydrogel pendant groups ionize and develop constant charges on the polymeric chains thereby triggering electro-repulsive forces necessary for pH-dependent swelling/deswelling mechanism (Kost, 1999). Little variations in environmental pH can result in a remarkable change in the mesh size of the hydrogel networks. The

pendant groups of cationic hydrogels ionized below the pKa of the hydrogel network resulting in swelling of the hydrogel at pH below the polymer pKa due to the osmotic pressure generated by the presence of ions within the system. However, the reverse is the case for anionic hydrogels, which swell at pH above the polymer pKa. Figure 7 is an illustration of mechanistic swelling of ionic hydrogels in alkaline and acidic media:

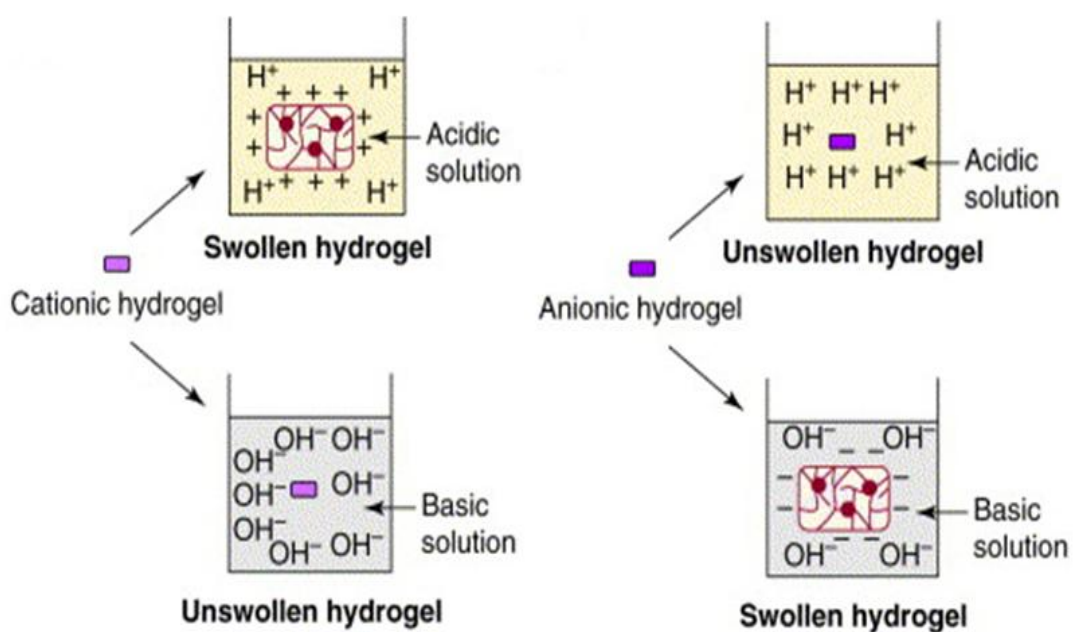


Figure 7. A pictorial representation of pH-sensitive swelling of ionic hydrogels (Gupta et al., 2002)

The main parameters that influence the swelling degree of ionic hydrogels include the properties of the swelling medium (ionic strength, counter ion and pH) and those of the polymer (degree of ionization, charge, pKa of the ionizable functional groups, concentration, hydrophobicity/hydrophilicity and crosslinking density) as reported by (Gupta et al., 2002). Additionally, the hydrogel swelling kinetics has been reported to be influenced by the type of the buffering species (Fig.8).

Gupta et al., (2002), reported that swelling of hydrogels in solutions buffered with monovalent anions were found higher than those buffered with multivalent anions

(phosphate, citrate, etc.) when the solution pH and ionic strength are constant. Gupta et al., (2002) also reported that swelling of the hydrogel in buffered solutions containing weak organic acids reached equilibrium faster as compared with that in unbuffered media. In this research work, chitosan and polyvinyl alcohol containing amine and hydroxyl groups were used as the functional polymers to obtain pH-sensitive hydrogels. The hydrogel is expected to swell under acidic media and deswells in basic solutions.

2.1.1.2 Glucose-sensitive Hydrogels

Glucose-sensitive hydrogel based systems are potentially appropriate to the development of self-modulated insulin delivery system, and with the manipulation of chemical integrity of such hydrogels, they can be fabricated to undergo volume variations in response to changes in blood glucose level. These hydrogels can shrink or swell in accordance to blood glucose concentration (Hoffman, 2002; Kim, 2011). Based on this fact, various glucose-sensitive hydrogels have been designed for regulating insulin delivery and monitoring glucose levels (Fig. 7).

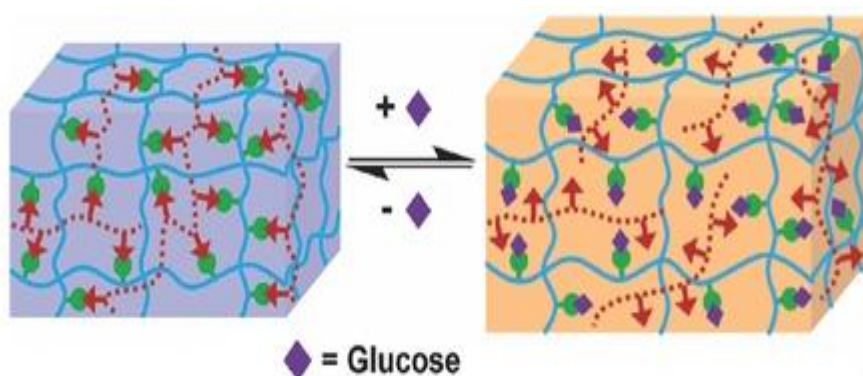


Figure 8. Pictorial representation of glucose-sensitive hydrogels

Until now, three main classes of glucose-sensitive hydrogels have been reported and described as follows (Fig. 8):

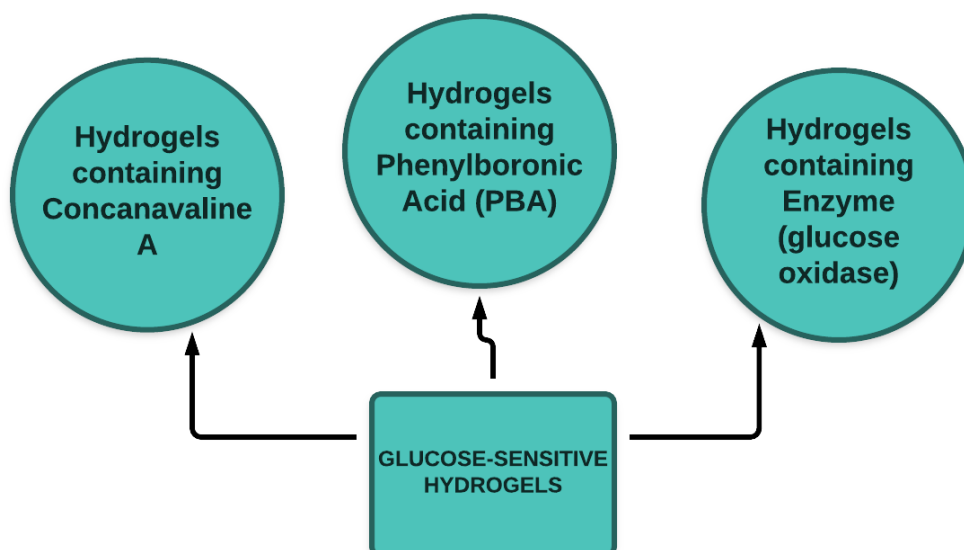


Figure 9. Three main classes of glucose-sensitive hydrogels

Hydrogels containing Concanavalin-A (Con-A) can undergo sol-gel phase transitions according to the glucose concentration in the medium. The Con-A acts as a crosslinker and, due to the non-covalent interaction between Con-A and glucose, reversible crosslinks are formed. The mechanism of Con-A based glucose-sensitive hydrogel can be explained as follows; glucose molecules compete with pendant molecules as they diffuse into the polymer network, then bind to the Con-A sites, thereby releasing the crosslinks and resulting in the swelling of the hydrogel. Hence, insulin release can be regulated as a function of the glucose concentration within the system. Meanwhile, leakage of Con-A has been reported. Thus, this degrades device function, introduces toxicity and limits the overall application of Con-A based glucose-sensitive hydrogels.

The second group is the enzyme-based (glucose oxidase) glucose sensitive hydrogels, and the glucose oxidase (GO-x) is the most extensively investigated enzyme for glucose sensors. Several investigators have developed insulin delivery system via the combination of GO-x with pH-responsive hydrogels. In this approach,

GO-x is immobilized within the pH-responsive hydrogel. In the presence of glucose, the immobilized GO-x catalyzed the glucose and produced gluconic acid, hence reducing the pH of the system and causing the hydrogel to swell. Therefore, insulin is released as the permeability of the pH-responsive hydrogel changes (Kost et al., 1999).

As opposed to the studies that utilize Con-A or glucose oxidase, incorporation of phenylboronic acid (PBA) within a polymeric network is the third approach to constructing a G-SH based system. In this approach, totally synthetic G-SHs systems involving no biological components are obtained using PBA. The PBA can react with polyols (glucose and fructose) to form reversible complexes in aqueous media (Fig.9). However, this reversible complex can be disrupted by a co-existing polyol by forming a more stable complex (Lin, 2010).

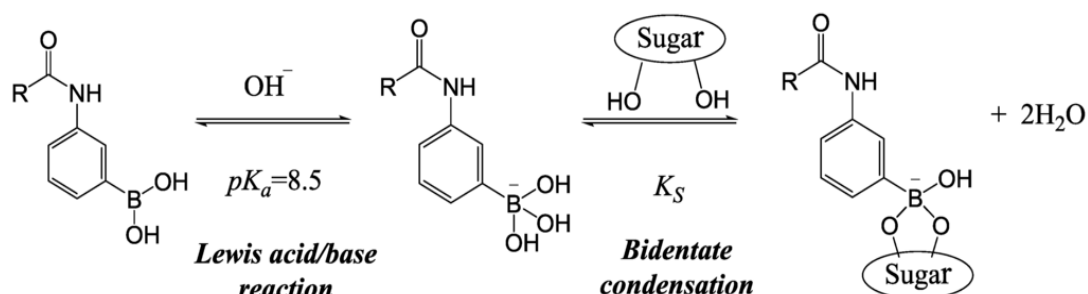


Figure 10. Complex between a sugar molecule and PBA moiety in aqueous solution (Lin, 2010)

As represented in Fig. 9, boron species under basic conditions becomes negatively charged by Lewis acid-base reaction, and then sugar molecules with planar diols stabilized the charge formed via complex formation. At physiological pH, sugars such as fructose and glucose bind with the PBA moiety; however, glucose does not bind as strongly as fructose. Indicating that at physiological pH, PBA lacks glucose

specificity. Meanwhile, PBA moiety is charged above its pKa ($> \text{pH } 10$) and can specifically complex with two glucose molecules forming a bridge on separate chains (Lin, 2010).

Although the enzyme based G-SHs exhibit high specificity and sensitivity to glucose, they suffer from several limitations. For instance, the reaction continuously produces hydrogen peroxide, consumes targeted analyte and glucose. Hence, the consumptive process affects the measured glucose value (Peppas, 2004). Unlike the GOx-GHs system, con-A based G-SHs are non-consumptive process but the typical competitive glucose binding system. Therefore, con-A based G-SHs are expected to be stable since they can sense an equilibrium glucose concentration. Meanwhile, Con-A system has been reported to be toxic and immunogenic (Kim et al., 2014). Reports had shown that boronic acid is a biocompatible material with low toxicity and low immunogenicity. Therefore, PBA based glucose sensors are highly suitable for long-term use.

2.2 Chitosan Based Hydrogel systems for different biomedical application

Chitosan is a linear polysaccharide composed of randomly distributed β -(1-4)-linked D-glucosamine (deacetylated unit) and N-acetyl-D-glucosamine (acetylated unit). It is made by treating shrimp and other crustacean shells with the alkali sodium hydroxide. Chitosan have unique characteristics that distinguish them from the other natural polymers because of their biodegradable, environmental friendly (nontoxic compound) natures. Chitosan is available in nature and estimated as the second most abundant polysaccharide after Cellulose.

The chitosan possessed many interesting chemical characteristics because of the two hydroxyl groups and one amine group, both of these groups allowed chitosan to be modified to produce many derivatives. These derivatives have different wonderful applications with various characteristics. Chitosan have shown peculiar properties such as biodegradability, biocompatibility, bioactivity, selective permeability, polyelectrolic action, chelation, ion exchange properties, antitumor and antimicrobial activity.

Zhao et al they prepared Hydrogels from poly(vinyl alcohol) (PVA) and carboxymethylated chitosan with electron beam irradiation at room temperature. Then they investigate the antimicrobial activity of the hydrogels against *E. coli* bacteria via optical density method. The blend hydrogels exhibited satisfying antibacterial activity against *E. coli* (Zhao, Mitomo, Zhai, Yoshii, Nagasawa, & Kume, 2003)

Koyano et al they synthesized hydrogels by blending of poly(vinyl alcohol) (PVA) and chitosan in varying proportions. They found that the increasing water-contact angle on the hydrogel surface with increasing chitosan content indicated that the chitosan molecules were more hydrophobic than were PVA molecules. (Koyano, Koshizakib, Umeharab, Nagurac, & Minoura, 2000)

Nho et al they synthesized hydrogels for wound dressing, the synthesized hydrogel were prepared from a mixture of chitosan and polyvinyl alcohol (PVA)/poly-N-vinylpyrrolidone (PVP) by freeze thawing method, gamma-ray irradiation, or combined freeze thawing and gamma-ray irradiation. The physical properties of the hydrogels, such as gelation and gel strength, were higher when the combination of

freezing and thawing and irradiation were used rather than just freeze thawing. The PVA/PVP–chitosan composition and irradiation dose had a greater influence on swelling than gel content. Swelling percent increased as the composition of chitosan in PVA/PVP–chitosan increased (Nho & Park, 2002)

γ -Irradiation combined with freeze-thawing, was another method was applied by Yang and his team, the synthesized product was used for wound dressing. (Yanga, Liu , Chen, Yua , & Zhu, 2008)

Grafting chitosan with PVA is also widely used by researcher, Kweon et al they produced Chitosan-g-poly(vinyl alcohol) (PVA) copolymers with different grafting percent were prepared by grafting water-soluble PVA onto chitosan. The drug-release behavior was studied using the synthesized hydrogel copolymer matrix containing prednisolone in a drug-delivery system under various conditions. (Kweon & Kang, 1999)

Nafee et al were apply Mucoadhesive patches for delivery of cetylpyridinium chloride (CPC), they used polyvinyl alcohol (PVA), hydroxyethyl cellulose (HEC) and chitosan. They used plain and medicated patches for Swelling and bioadhesive characteristics (Nafee , Boraie , Ismail , & Mortada , 2003)

Sajeev et al prepared polyvinyl alcohol (PVA) in aqueous solution, the prepared compound was studied as a function of applied potential, tip-target distance and solution flow rate. Solutions of PVA and chitosan were homogeneously mixed and electrospun to result in blend nanofibres and their properties were investigated. (Sajeev, Anoop Anand, Menon, & Nair, 2008)

Blend membrane consisting of poly(vinyl alcohol) (PVA) and chitosan was prepared from a solvent-casting technique by Kim et al, FTIR and X-ray diffraction methods were used for characterization. They found that the cross-linking the blend with glutaraldehyde produces a membrane with lower crystallinity and a smaller swelling degree, but having improved thermostability and mechanical properties. The prepared blend membrane shows a pH-dependent swelling characteristic. (Kim, Kim, Lee, & Kim, 1992)

One of the PVA/chitosan blended membrane was studied for cell culture by Chuang et al. Cells cultured on the PVA/chitosan blended membrane had good spreading, cytoplasm webbing and flattening and were more compacting than on the pure PVA membrane. Consequently, the PVA/chitosan blended membrane may spatially mediate cellular response that can promote cell attachment and growth, indicating the PVA/chitosan blended membrane should be useful as a biomaterial for cell culture. (Chuang, Young, Yao, & Chiu, 1999)

2.3 Drug Release Mechanism

Intensive research efforts have been committed to developing biocompatible drug delivery system due to rapidly increasing disease and health problems (Mahdavinia et al., 2014; Reddy et al., 2013). A drug release mechanism involves simultaneous absorption of fluid and desorption of the immobilized drug via a swelling mechanism (Figure 10).

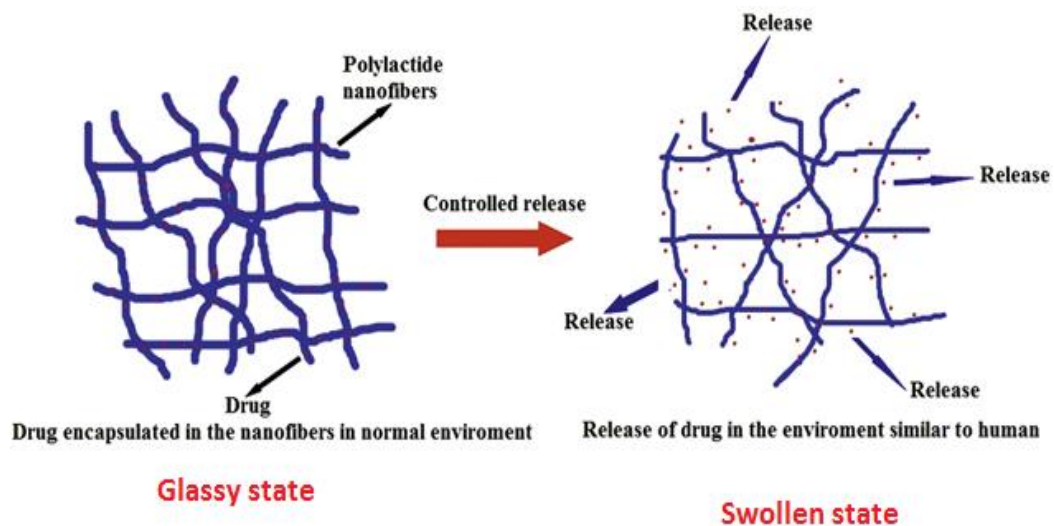


Figure 11. Pictorial representation of drug release mechanism

The hydrogels are mostly glassy when dehydrated, and but allows solvent penetration into free spaces when in contact with any thermodynamically compatible solution or water. When enough water/fluid has entered the hydrogel matrix, the glassy temperature of the hydrogel reduces to the experimental temperature. The presence of water/fluid within the glassy hydrogel results in internal stresses, then increases in the end-to-end distance and radius of gyration of the polymer molecules is observed. Finally macroscopical swelling is seen.

The transport of water/fluid into the glassy hydrogel matrix occurs within a clearly described velocity front and a synchronic increase in the thickness of the swollen region. Such mechanism of swelling and diffusion mostly do not follow a Fickian diffusion model (Gupta et al., 2002). The rate-controlling parameter conciliating drug delivery is the resistance of the hydrogel to change in shape and increase in volume. Diabetes is a manageable disease, which requires frequent and accurate measurements of a patient's glucose levels to ensure they stay within a permitted range (Peppas, 2004). It has been reported that diabetics still suffer from

hyperglycemic and hypoglycemic series as a result of the fluctuation of glucose levels (Peppas, 2004). It is particularly important to develop biocompatible drug delivery systems that are sensitive to fluctuations in blood glucose level.

2.4 Hydrogels as Antimicrobial Agents

Nowadays, there has been increasing interest on the application of hydrogel for several antimicrobial applications (antibacterial coatings, skin bactericide, wound dressings, etc.) and as a host in various drug delivery matrices (Zou et al., 2015). Recently, the antimicrobial activities of chitosan and its derivatives against various microorganisms (yeast, bacteria, and fungi) have received substantial attention (Benhabiles et al., 2012; Limam et al., 2011).

There are three mechanisms that have been proposed as the cause of the inhibition of microbial cell membranes by chitosan, and the most acceptable being the interaction between the negatively charged microbial cells and protonated NH_3^+ functional groups on chitosan molecules.

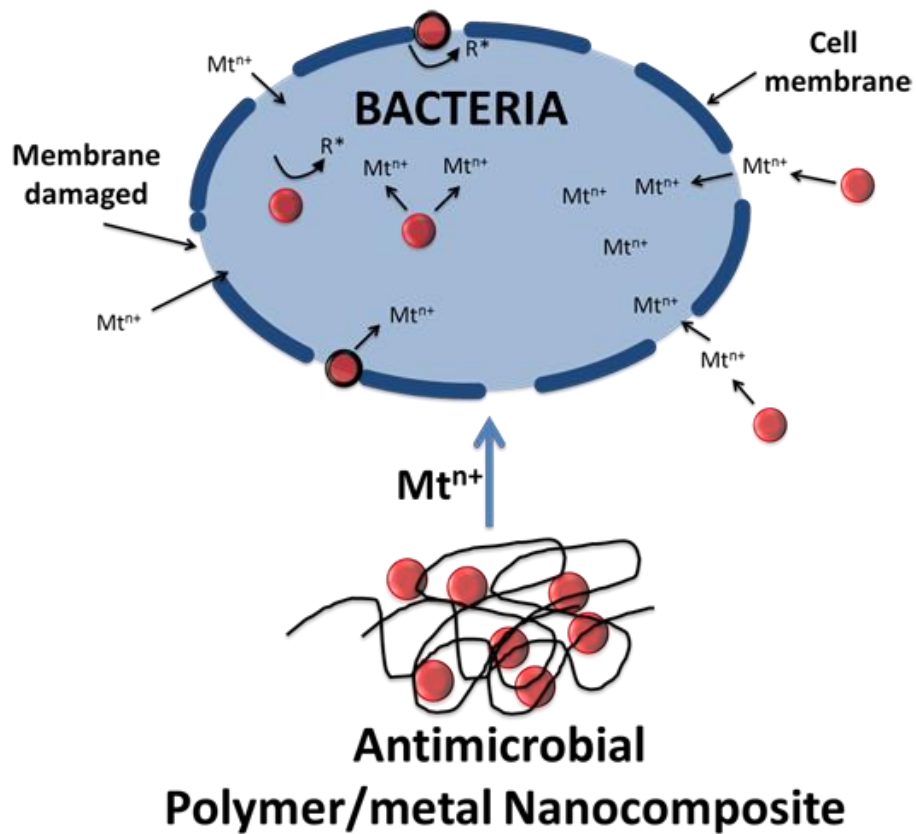


Figure 12. Antibacterial mechanism of polymer composite

The second acceptable model is blocking of RNA transcription from DNA via sorption of chitosan molecules into the DNA. The antimicrobial activities of chitosan-based hydrogel are considerably based on the chitosan physical characteristics, such as: (degree of deacetylation and molecular weight). Here, boric acid crosslinked chitosan/PVA was tested for antimicrobial activities, and the obtained results are inspiring.

Chapter 3

EXPERIMENTAL

3.1 Chemicals and Materials

All the chemicals used were of reagent grade. Chitosan (medium molecular weight with 85% degree of deacetylation) was supplied by Sigma–Aldrich (Germany). PVA (99% hydrolyzed and MW: 72000 g/mol), boric acid and acetic acid were obtained from Merck (UK). Aqueous solutions were all prepared with deionized water. The simulated intestinal fluids (phosphate buffer solutions (PBS): pH 7.4) were prepared as described elsewhere (Das et al., 2014) and ionic strength of the solutions were adjusted to ≈ 0.1 M using sodium chloride.

3.2 Synthesis of Boric acid cross-linked Chitosan/PVA hydrogel

Chitosan/polyvinyl alcohol hydrogel (CS–PVA) was prepared via a boric acid cross-linking technique in combination with an alternate freeze–thawed process (Wang et al., 2013). Chitosan (CS) was dissolved in aqueous acetic acid (2% v/v); then, 49 mL of the CS solution was mixed with 4.2 mL of PVA aqueous solution (10%) and stirred mechanically at 25 °C for 3 h. After a homogeneous solution was obtained, 2 mL of boric acid aqueous solution (25%) was added slowly in a drop wise fashion into the mixture and continuously stirred for another 4 h to obtain a homogeneous gel. The gel was kept frozen at -20 °C for 24 h. Subsequently, the frozen gel was thawed at 25 °C for 6 h. The CS–PVA hydrogel was obtained after three freeze–thawed cycles, immersed in a dilute NaOH solution to neutralize the excess acetic

acid, and then washed several times with deionized water. The dehydrated hydrogel was dried in an oven at 70 °C.

3.3 Characterization

FTIR absorption spectra of CS, PVA, and CS–PVA hydrogel were taken on a Fourier-transform infrared (FTIR) spectrometer (PerkinElmer, 65 FT-IR Spectrometer, USA) over the region from 400 to 4000 cm^{-1} . The surface morphology of the hydrogel was observed using a scanning electron microscope (SEM) (JEOL JSM-6360LV, Japan) at an accelerating voltage of 20 kV for 75 sec after coating the sample with a gold film.

3.4 Swelling Studies

The gravimetric method was employed to determine the swelling and equilibrium data of the hydrogels. Briefly, the hydrogels were immersed in given solutions, withdrawn at particular time intervals, gently dried with filter paper and then weighed on an analytical balance to determine the swelling ratio. The equilibrium swelling ratio was determined when the weight of the swollen hydrogel was constant. The swelling studies were conducted in triplicate, average results reported and the swelling ratio was determined as follows:

$$Q_e (g / g) = \frac{W_{wet} - W_{dry}}{W_{dry}} \quad (1)$$

3.5 Drug Release Experiments and Optimization

Insulin and Bovine serum albumin (BSA) were selected as model drugs. The loading of the drugs into CS–PVA hydrogel network was done via swelling equilibrium method. Briefly, the hydrogels were allowed to swell in 1–5 mg/mL aqueous solutions of insulin/BSA for 72 h at 5°C and then dried to obtain the drug-loaded hydrogel.

The drug release experiments were performed by immersing drug-loaded hydrogel in 50 mL of phosphate buffer, pH 7.4 for 24 h with occasionally shaking at 37 ± 0.2 °C. Aliquots of the solution were removed at pre-determined time intervals and insulin/BSA concentrations in the unknown samples were quantified using UV-Vis spectrophotometer (UV-Win 5.0, Beijing, T80+) at 280 nm. All release experiments were performed in triplicate, and the cumulative drug release was calculated.

Response surface methodology (RSM) is a proficient approach in the prediction of drug release and optimization of drug delivery devices (Das et al., 2013; Oladipo and Gazi, 2014b). Here, the influences of operating factors (pH, time, dosage and glucose concentration) on responses (loading efficiency and cumulative release (CR%)) were examined by RSM. A total of 20 experimental runs were proposed by SigmaXL (Ver. 7.0, Canada) for the independent variables and the matrix of the design including investigated responses are presented.

3.6 CS–PVA Hydrogel Antibacterial Test

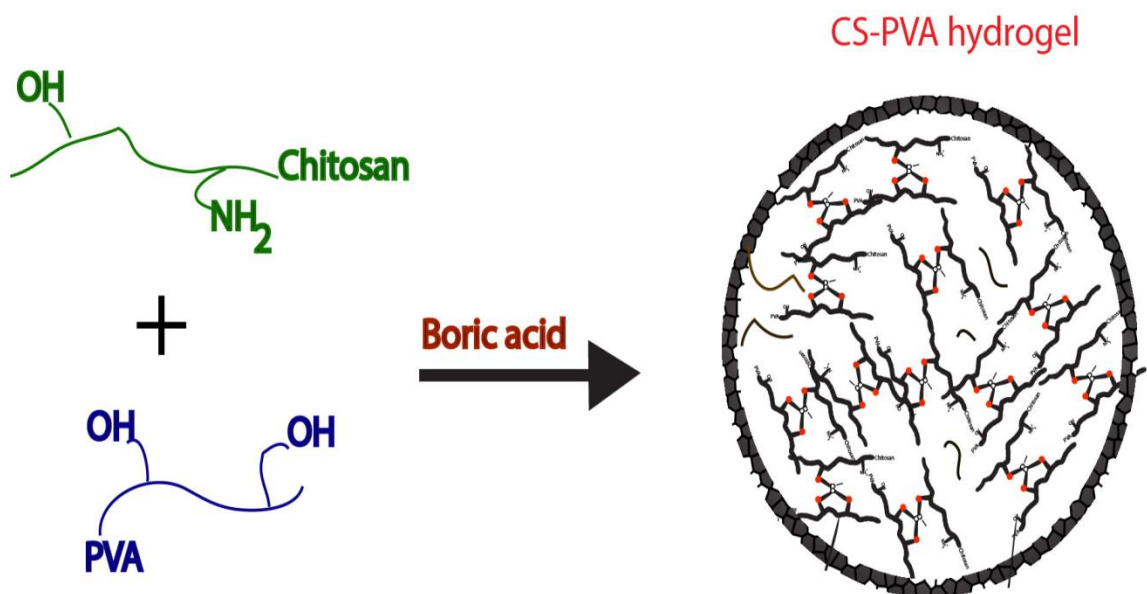
The antibacterial activity of the CS–PVA hydrogel was tested against *E. coli* (gram-negative) strain in nutrient agar medium. The agar plate was inoculated in 10 μ L of microbial suspension under a rotary shaker at 150 rpm. 10 mg of swollen hydrogel was transferred into the microbial agar plate and incubated for 16 h at 37°C. The cells were centrifuged at the mid-log phase, washed three times and re-introduced into the phosphate buffer solution (2%). The final cell concentration was obtained at 600 nm using Varioskan Reader. Pure CS–PVA hydrogel was utilized for control tests.

Chapter 4

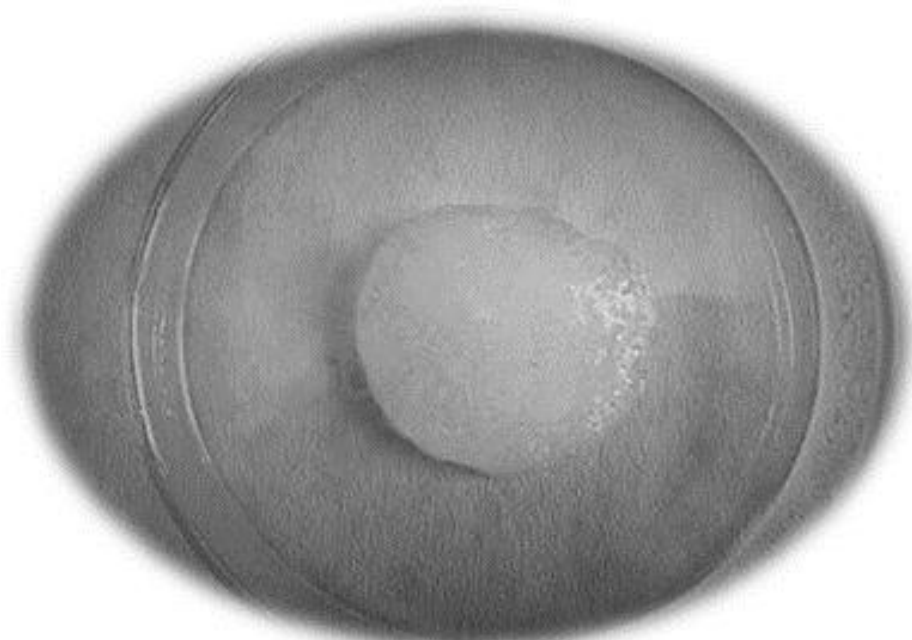
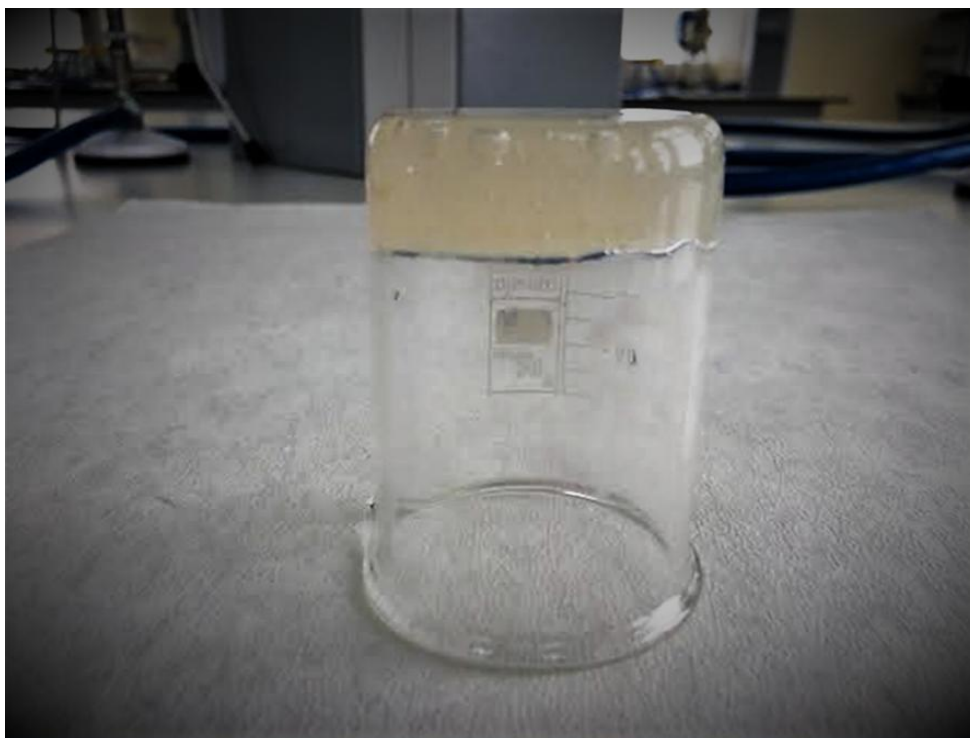
RESULT AND DISCUSSIONS

4.1 Synthesis and Characterization of Hydrogels

The chemical structures of CS, PVA and synthesis route of CS–PVA hydrogel are shown in Scheme 1. In the present work, a stable hydrogel with glucose-sensitivity was obtained using boric acid as a crosslinker and alternate freeze-thawed process (Scheme 2). The ratio of cross-linking was calculated according to the tri-functionality of boric acid.



Scheme 1. Synthesis route for boric acid crosslinked CS–PVA hydrogel



Scheme 2. Picture of the synthesized CS–PVA hydrogel

The FTIR of the samples is shown in Fig. 12. The pure PVA showed main absorption peaks at 3412 cm^{-1} (–OH stretching), 2862 cm^{-1} (–CH stretching), 1419 cm^{-1} (–CH bending) and 1093 cm^{-1} (–C–O– stretching). In the FTIR spectrum of chitosan, the

absorption peaks at 1648 cm^{-1} and 1562 cm^{-1} , are attributed to amide I and II peaks, respectively. The broad peak at 892 cm^{-1} , 1092 cm^{-1} indicates saccharine structure; the -C-O- stretching vibration respectively and peak at 2928 cm^{-1} is typical -CH stretching vibrations. The broad peak at 3380 cm^{-1} is attributed -OH and -NH symmetrical vibration.

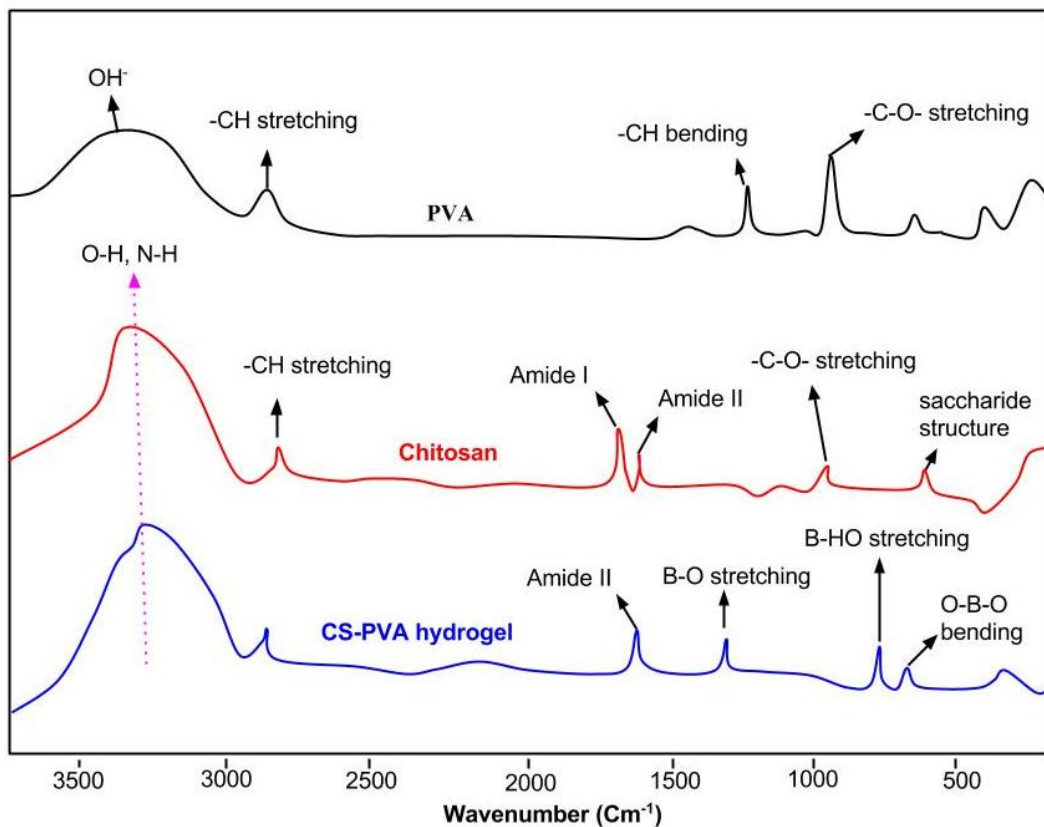


Figure 13. FTIR spectrum of CS, PVA and CS–PVA hydrogel

In the FTIR spectrum of the CS–PVA hydrogel, the characteristics peaks of PVA and chitosan are apparent and the broad band in the $3380\text{--}3412\text{ cm}^{-1}$ regions corresponding to the stretching vibrations of hydrogen bonded O-H and N-H obviously shifted to lower wavenumbers. This suggested that there was a crosslinking reaction between hydroxyl groups in PVA, CS chains and borate molecules (Oladipo and Gazi, 2014a; Uslu et al., 2008). Also, the appearance of new

peaks at 673, 761 and 1409 cm^{-1} is attributed to O–B–O bending, B–OH stretching and B–O stretching, respectively (Uslu et al., 2008). The SEM photographs of CS–PVA hydrogel and optimized BSA-loaded hydrogel are shown in Fig. 13 and 14, respectively. As seen in the SEM image of CS–PVA hydrogel, a denser morphology, wrinkles and tightly interconnected pores different from the porous structure of other published reports are seen (Wang et al., 2010). Water molecules can easily be transported into the CS–PVA hydrogel due to the presence of numerous interconnected tight pores in the hydrogel network.

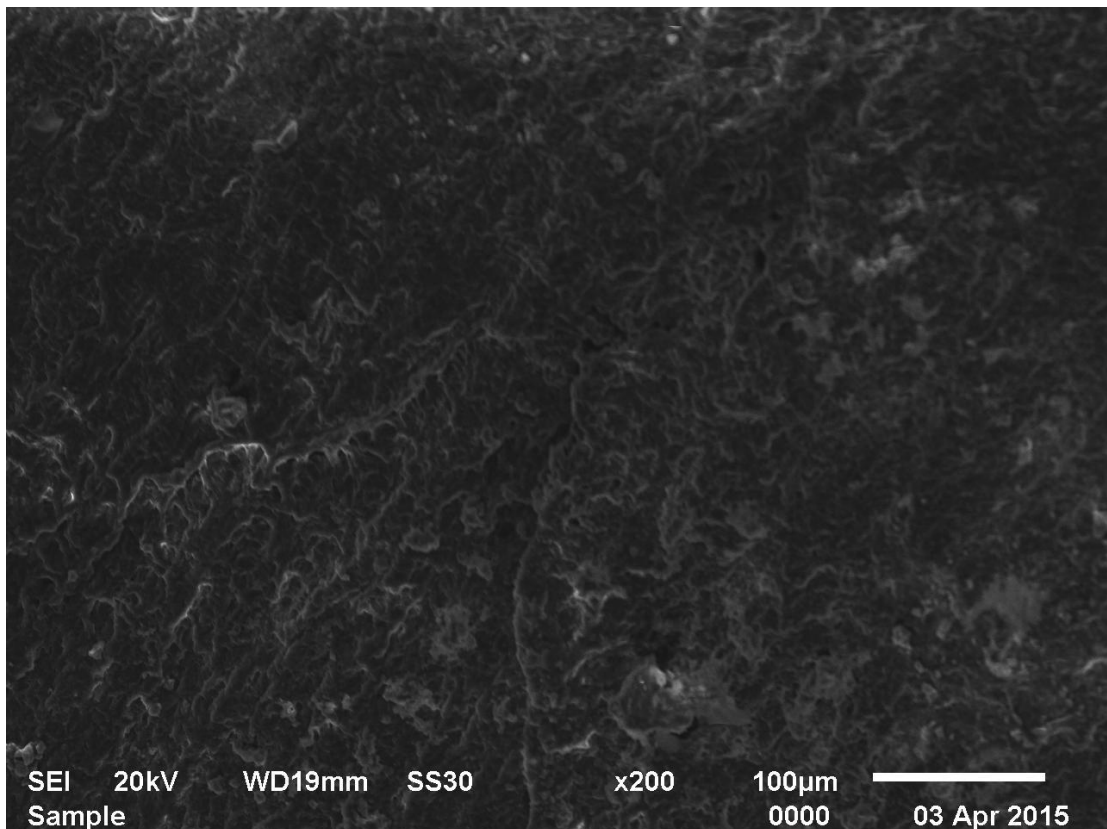


Figure 14. SEM image of CS–PVA hydrogel

The micrograph of the BSA-loaded gel showed a rough surface with severe wrinkles that may be attributed to partial collapsing of the polymeric network while drying (Matricardiet al., 2006). Some stripes of BSA particles are seen adhered to the

surface of the loaded hydrogel and network structure is less obvious compared with unloaded CS–PVA hydrogel.

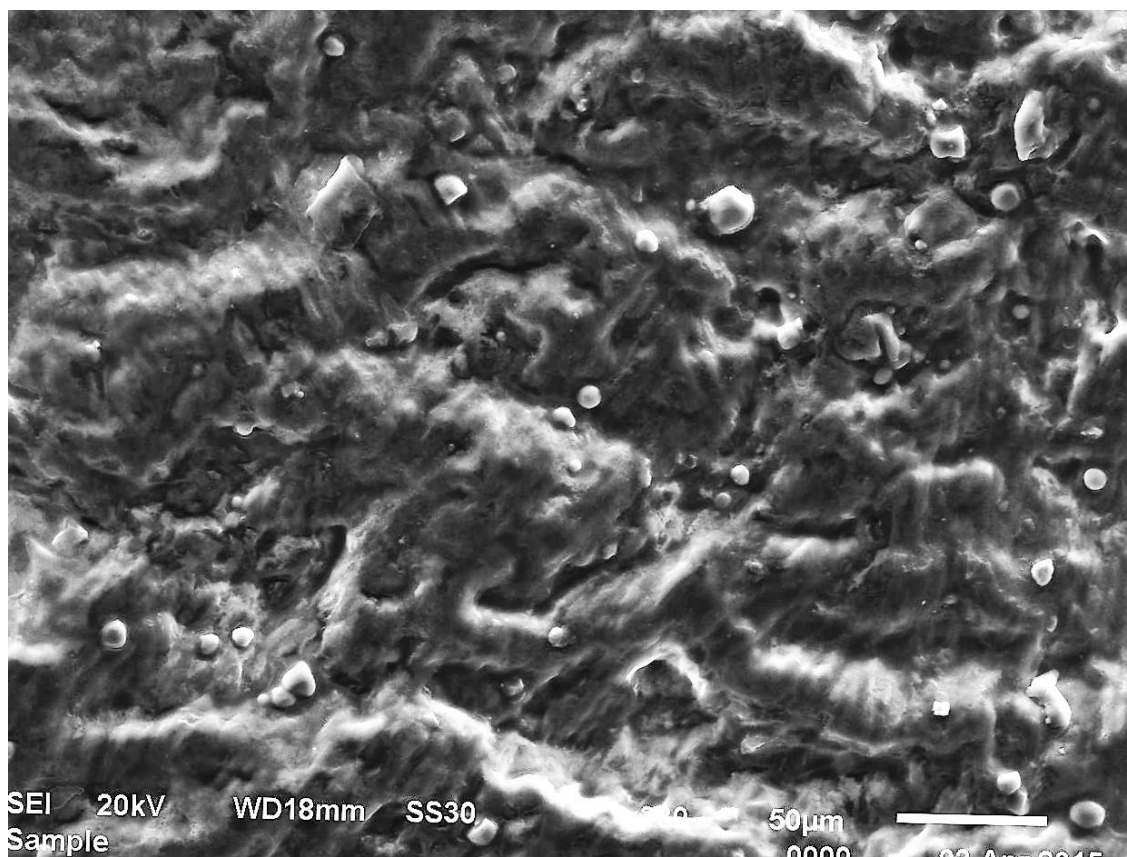


Figure 15. SEM photographs of optimized BSA-loaded hydrogel

4.2 Swelling Properties of CS–PVA Hydrogels and pH Sensitivity

The swelling ratio of the CS–PVA hydrogel was investigated in distilled water, acidic and basic environments to simulate the possible effect of pH on drug release. As shown in Figure 15, the swelling ratio is affected by the pH of the swelling media and this effect can be ascribed to the amino groups in the hydrogel network structure. It is evident that in the initial swelling stage, the CS–PVA hydrogel absorbed solvent rapidly, and then the swelling ratio increased moderately with time, and finally reached equilibrium in about 160 min. In the acidic environment, the weight of CS–

PVA hydrogel increased by about 0.5 folds during the initial 100 min in solution, but no significant swelling was observed after 160 min.

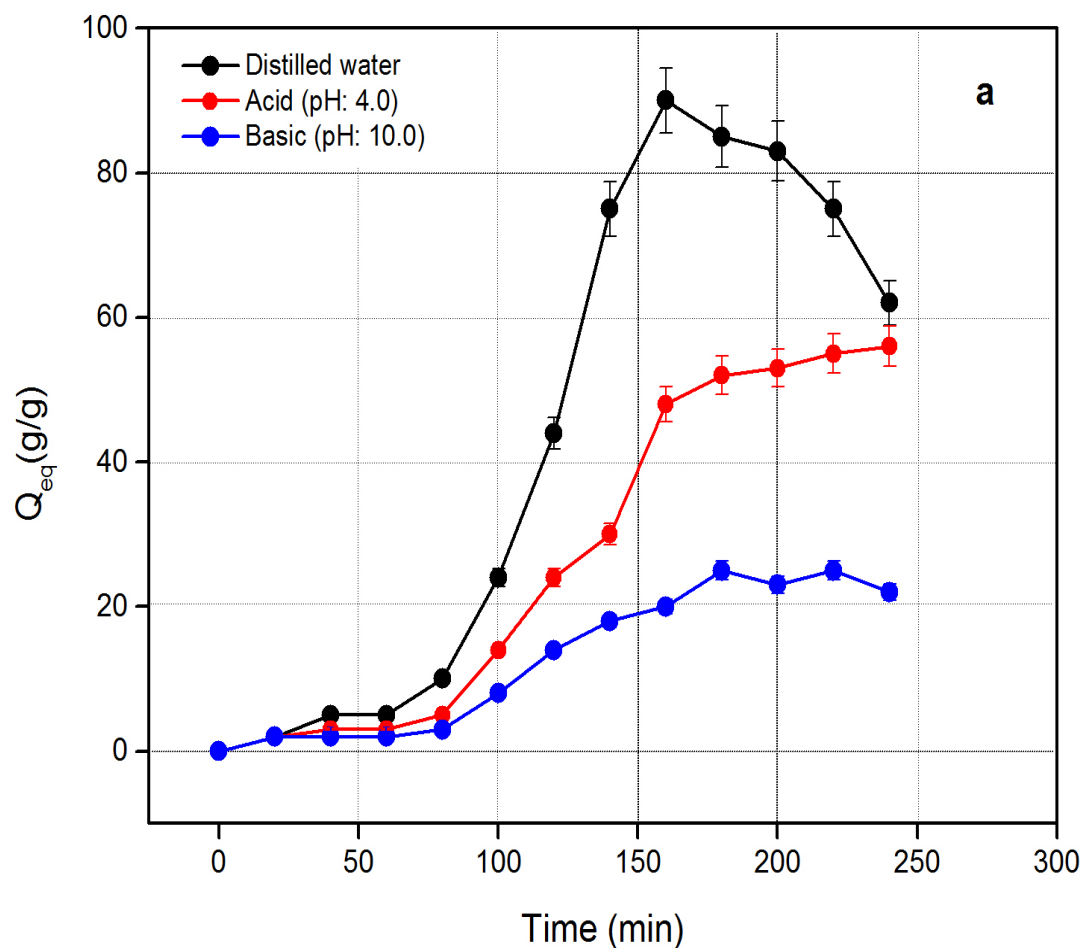


Figure 16. Swelling ratio of CS–PVA hydrogel in distilled water, acid, and basic media

The amino groups in the polymeric structure are charged when the swelling media is acidic, which leads to electrostatic repulsion between the polymer chains (Islam et al., 2013).

As obtained, the swelling ratio of CS–PVA hydrogel is higher at acidic pH (pH 4.0) than at basic solution (pH 10.0), which was due to the competitive expansion of the

positive hydrogel chains. The expansive polymeric network permitted more acid solution into the polymer interior (Zou et al., 2015).

It is evident that the swelling degree of the hydrogel in distilled water was much higher than that in pH 10 and pH 4, indicating a pH-sensitive swelling behavior. In distilled water, the polymer–water interactions predominate over the polymer–polymer interactions. As a result, the swelling ratio of the hydrogel is relatively high. Boric acid is a Lewis acid ($pK_a \approx 9.2$).

Therefore, in the region more alkaline than pH 9, more compact hydrogel network is formed due to hydrogen bond formed between $B(OH)_4^-$ and four hydroxyl groups, resulting in less swelling degree (Mahdavinia et al., 2014; Nayak et al., 2013). Fick's diffusion model was applied to investigate the transport mechanism of solvent into the hydrogels network according to the following equation (Evren et al. 2014):

$$F = kt^n \tag{2}$$

In this equation k is related to the network structure, F is fractional uptake at time t , and n is indicative of the transport mechanism. Fick's model associates the diffusive flow to the concentration in a steady state. According to Fick, the rate of flow of a solvent goes from regions of high concentration to that of low concentration, with a magnitude that is relative to the concentration gradient. A value of $n = 0.45 < n < 0.9$ represents non-Fickian diffusion, $n = 0.45$; represents Fickian diffusion (Case I), and $n = 0.9$ represents Case II transport mechanism (Mujtaba et al., 2014).

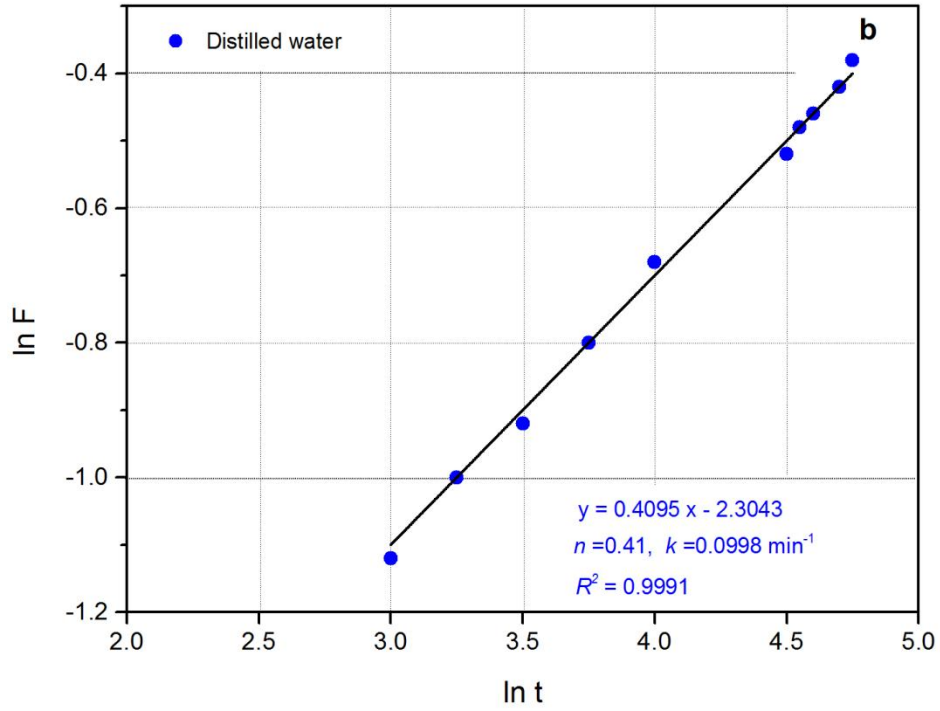


Figure 17. Pseudo-Fickian plot for fractional uptake of water by CS-PVA hydrogel

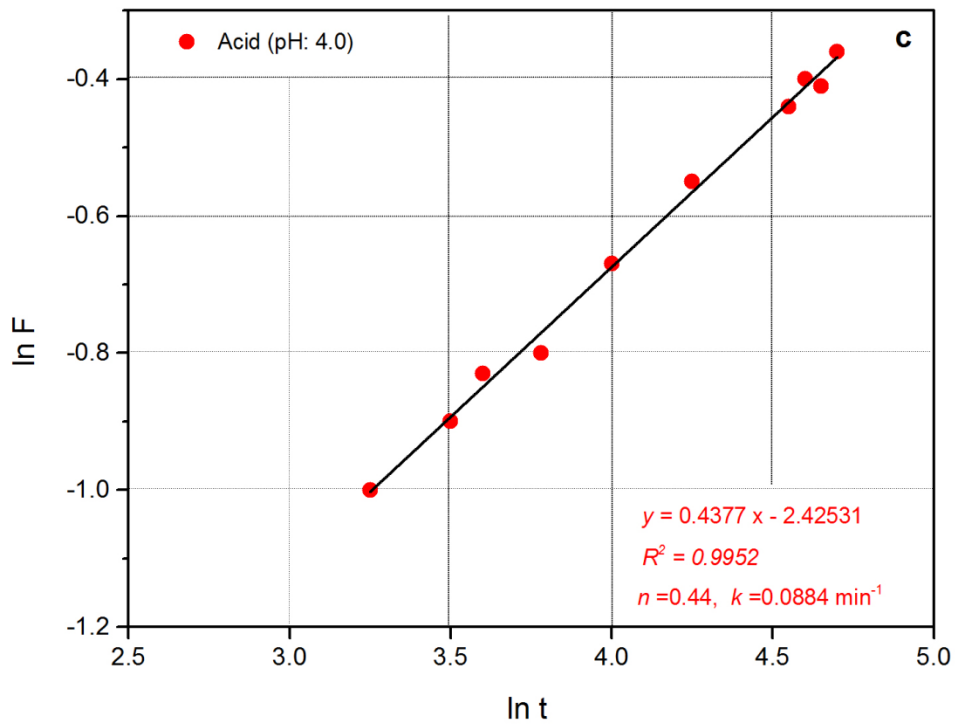


Figure 18. Pseudo-Fickian plot for fractional uptake of acid solution by CS-PVA hydrogel

The plots of $\ln F$ versus $\ln t$ are shown in Figure 16-18; k and the exponent n were calculated from the intercepts and slopes, respectively. As shown in Figure 3b-d, the values of n are less than 0.5 (0.34–0.44). Hence, the transport mechanism of the swelling media into the hydrogels is assumed to be pseudo-Fickian in nature.

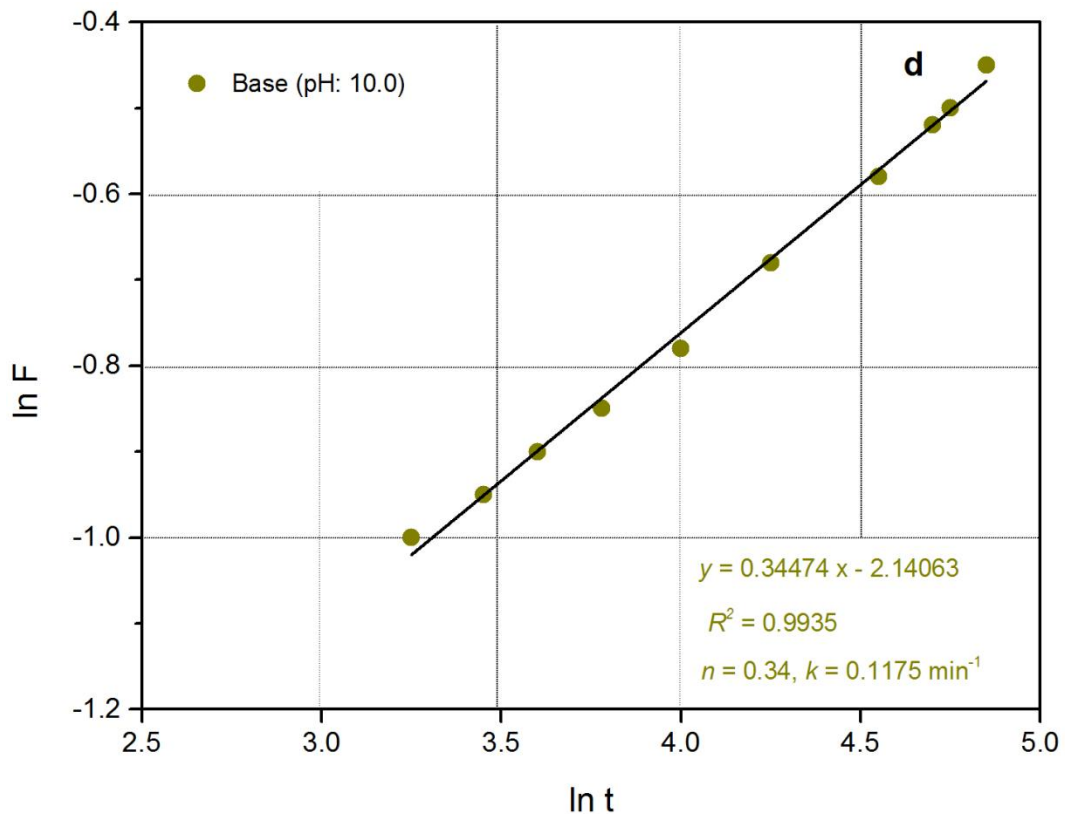


Figure 19. Pseudo-Fickian plot for uptake of basic solution by CS-PVA hydrogel

4.3 Glucose-sensitivity of CS-PVA Hydrogel

Buffers play a significant role in influencing binding constants between diols and boric acids (Matricardi et al., 2006; Wang et al., 2010). Phosphate buffer saline (PBS) is commonly used to simulate physiological conditions for biological applications. The pH-sensitive CS-PVA hydrogels may be applied as glucose-sensitive drug release system; therefore, the swelling behavior of CS-PVA hydrogel

was investigated by immersing the hydrogel in PBS (pH 7.4) at various glucose concentrations at 37 °C.

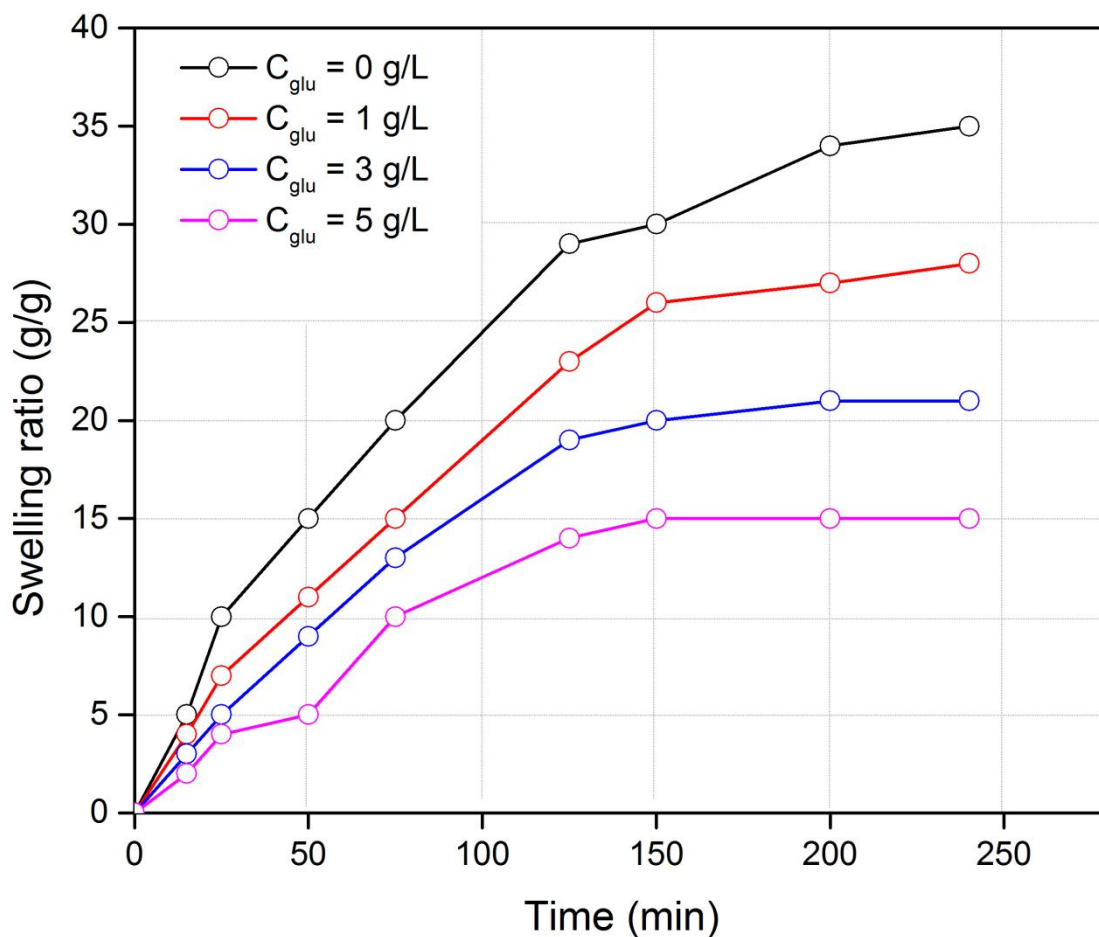
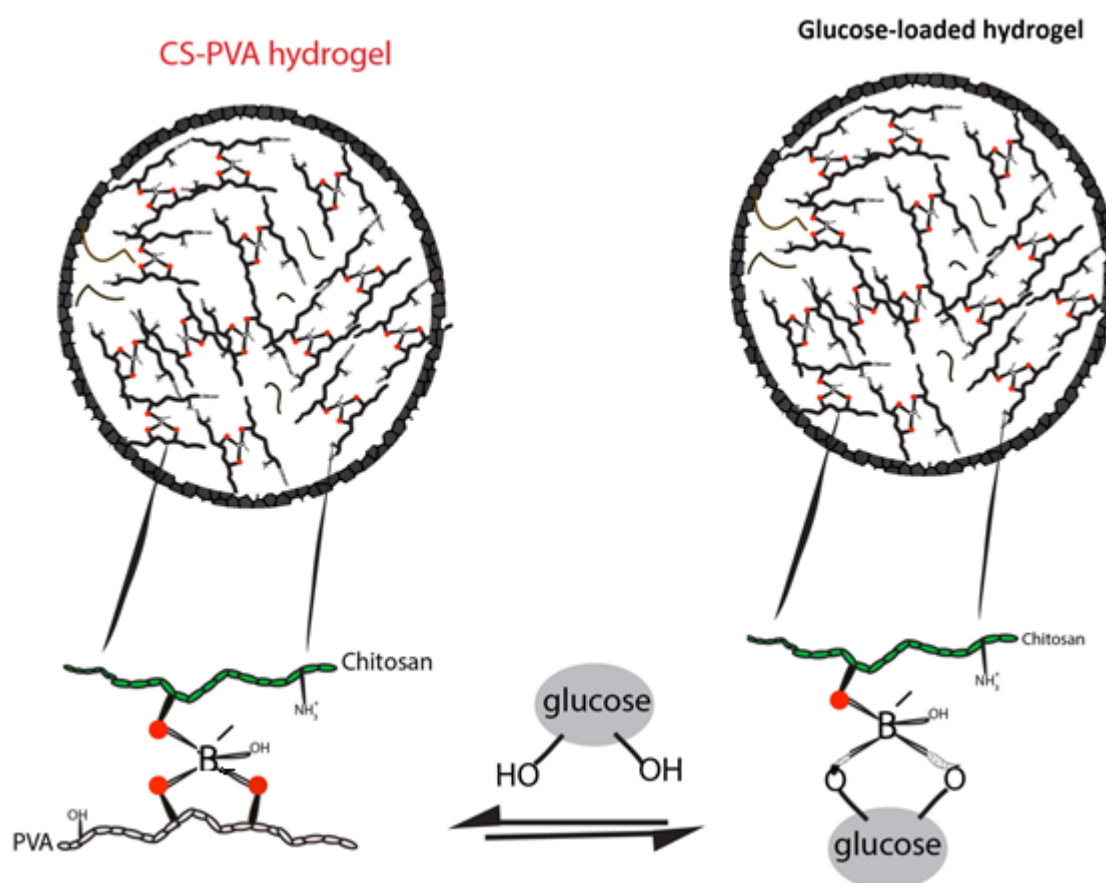


Figure 20. Swelling behavior of CS–PVA hydrogel in PBS (pH 7.4) at various glucose concentrations.

As expected (Figure 19), the hydrogel showed a rapid sensitivity for all glucose concentrations during the initial 120 min. The CS–PVA hydrogel swells with time in a pattern that depends on the glucose concentration in the medium, and after initial stage, the swelling rate slowed down, which can be ascribed to depleting functional binding sites on the hydrogel. In the control solutions (glucose = 0 g/L), it is important to stress that the hydrophilic nature of PVA in the hydrogel network is responsible for the swelling observed in the absence of glucose and these results are

consistent with the pH-sensitive test and earlier reports (Ivanov et al., 2004; 2014; Uslu et al., 2008).

As earlier reported, the boric acid moiety within the hydrogel network can form stable complexes with glucose even at physiological pH. It is known that monoborate anions complex polyols and organic *cis*-diols (Uslu et al., 2008), hence, glucose sensing using CS–PVA hydrogel is ascribed to complex formation between glucose and boric acid (Scheme 3).



Scheme 3. Mechanism of glucose complexation with CS–PVA hydrogel

The formation of charged complex increases the degree of ionization within the hydrogel network leading to an influx of counter-ions and solvent that swell the CS–PVA hydrogel. The hydrogel is also observed to swell more at PBS (pH 7.4) than in

PBS (pH 4.0). This observation may be attributed to the lowered amount of reactive monoborate, which leads to electrostatic repulsion between the protonated polymer chains at the acid media (Nayak et al., 2013; Wang et al., 2010).

4.4 Swelling Behavior of the CS–PVA Hydrogel in Physiological Fluids

The effects of double distilled water and simulated physiological fluids (urea solution(5g/100ml); glucose solution (5g/100ml), Hank’s solution; saline water (0.9 g NaCl/100 ml) and synthetic urine ((0.1 g MgSO₄ + 0.06 g CaCl₂ + 2 g urea + 0.8 g NaCl)/100ml) on the swelling of CS–PVA hydrogel were examined at 37 °C.

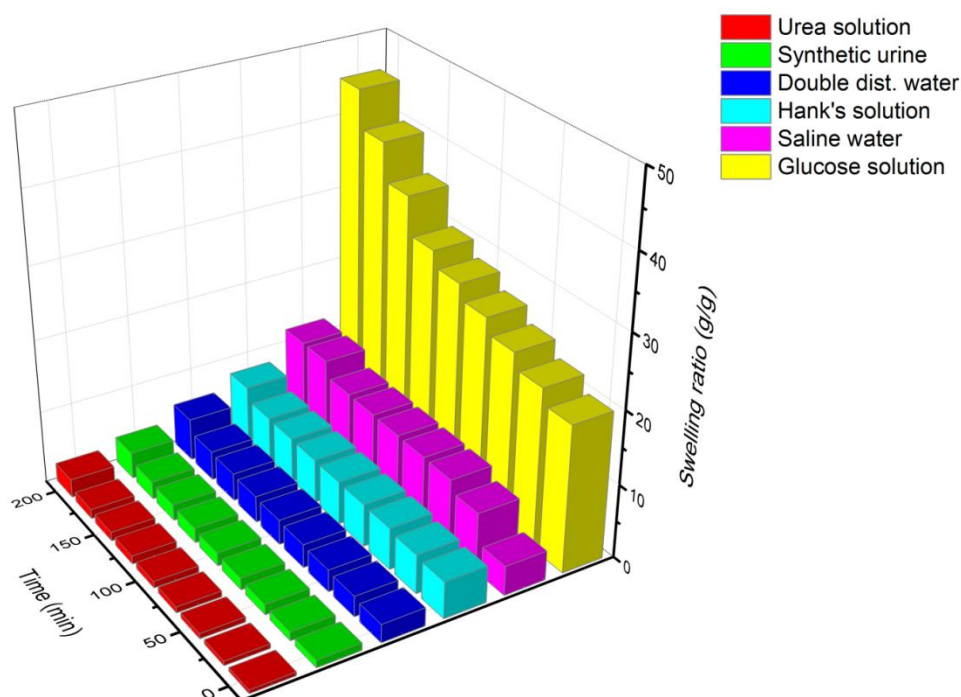


Figure 21. Swelling ratio of the CS–PVA hydrogel in physiological fluids

The result is shown in Fig. 20, the swelling of the gel in urea and synthetic urine solutions are similar to those of double distilled water. However, the swelling ratios of the gel in glucose solution are higher than the Hank’s and saline solutions. The

CS–PVA gel swelling mechanism in various physiological fluids can be said to be governed by Gibbs–Donnan equilibrium (Nayak et al., 2013). The interactions between glucose and borate induce a tilt in the charge equilibrium and, result in counter-ion osmotic pressure solution was attributed to strong competition between the borate in the hydrogel and the co-existing ions in the urea solution (Nayak et al., 2013).

4.5 Experimental Design for Drug Loading Efficiency and Capacity

The drug loading efficiency of the CS–PVA hydrogel system was evaluated by measuring the concentration of the initial drug loaded compared with the free drug remained in the dispersion buffered medium. The BSA or insulin molecules are assumed to be adsorbed via hydrogen bonding between NH₂ and/or hydroxyl groups of CS–PVA and carboxylate ions of BSA or insulin in the solution. Drug loading capacity (DC) and drug loading efficiency (DE) were calculated according to the following equations (Li et al., 2015):

$$DC = \frac{M_{\text{drug in CS-PVA}}}{M_{\text{drug in dispersion medium}}} \times 100 \quad (3)$$

$$DE = \frac{M_{\text{initial drug loaded}} - M_{\text{free drug}}}{M_{\text{initial drug added}}} \times 100 \quad (4)$$

The SigmaXL optimization software was utilized to find the best drug loading efficiency and capacity. Three factors (time, drug/CS–PVA ratios, and pH) RSM were applied to estimate their effect on the system's response for insulin (Figure 21) and BSA (Table 1).

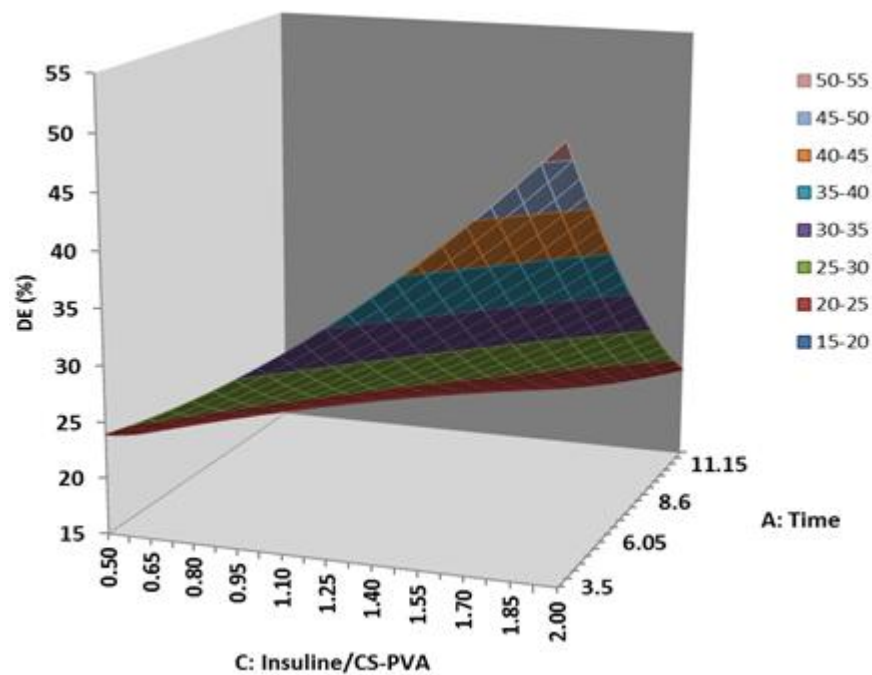
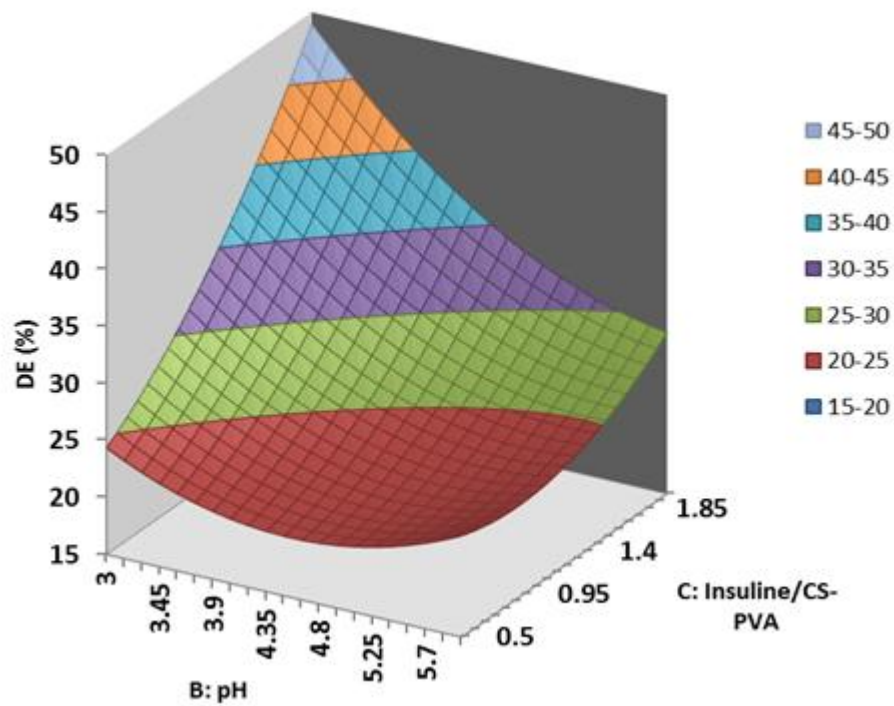


Figure 22. Response surface of the combined effects of pH, time and insulin/CS-PVA on drug loading efficiency.

The surface plots of pH and time on the loading efficiency at various insulin/CS-PVA ratios are shown in Figure 21. As evidently shown, decreasing pH and increasing of insulin/CS-PVA ratio, result in the higher amount of drug loading

efficiency. This could be as a result of increased interaction between the carboxylate ions of insulin and the protonated amine groups of the CS–PVA at lower pH. Similar results had been reported by Shafie and Fayek (2013), that pH value and drug/material ratio affected the loading efficiency. Also, similar observation was noted in the surface plot of insulin loading time with varying insulin/CS–PVA ratio. The insulin loading efficiency increased since the interaction between the insulin and the hydrogel is balanced over time.

Table 1. Experimental design layout for BSA loading and the obtained results

Run Order	Blocks	A: Time (h)	B: pH	C: BSA/CS-PVA	DE (%)	DC (%)
1	1	12	6	1.25	33.7	27.89
2	1	7.75	6	0.5	36.9	39.67
3	1	3.5	6	1.25	34.6	35.56
4	1	3.5	4.5	1.25	26.9	36.89
5	1	12	6	1.25	49.8	38.89
6	1	7.75	4.5	1.25	37.6	36.67
7	1	7.75	3	0.5	38.5	28.89
8	1	3.5	3	1.25	57.9	39.8
9	1	7.75	4	2.0	50.6	42.78
10	1	3.5	4.5	0.5	27.9	33.78
11	1	7.75	4.5	1.25	25.8	29.55
12	1	7.75	3	1.25	33.6	30.56
13	1	7.75	6	0.5	33.4	32.89
14	1	7.75	6	2.0	36	39.3
15	1	7.75	4.5	1.25	35.8	37.55
16	1	12	3	1.25	33.5	35.45
17	1	7.75	6	2.0	38.9	38.89
18	1	3.5	4.5	0.5	43.9	36.67
19	1	7.75	3	2.0	62.6	48.89
20	1	12	3	2.0	59.8	39.8

The application of RSM to BSA loading into CS–PVA yields a regression equation in terms of the operating factors (Eq. 5), which indicates an empirical relationship between the tested factors and the drug loading capacity.

$$\text{DC (\%)} = (24.81) + (-7.83) * \text{A: Time} + (-9.06) * \text{B: pH} + (8.46) * \text{C: BSA/CS-PVA} + (9.9) * \text{AB} + (-6.48) * \text{AC} + (-4.83) * \text{BC} + (2.37) * \text{AA} + (3.90) * \text{BB} + (2.86) * \text{CC}$$

Table 2. ANOVA for response surface quadratic model for BSA loading onto CS-PVA

Term	Coefficient	SE Coefficient	T	p-Value Prob >F	Significance
Constant	24.81666667	2.770002382	8.959	0.0000	Significant
A: Time	-7.83125	1.696273105	-4.617	0.0002	Significant
B: pH	-5.06875	1.696273105	-2.988	0.0073	Significant
C: BSA/CS-PVA	7.4625	1.696273105	4.399	0.0003	Significant
AB	9.9	2.398892431	4.127	0.0005	Significant
AC	-6.4875	2.398892431	-2.704	0.0136	Significant
BC	-4.8375	2.398892431	-2.017	0.0004	significant
AA	2.379166667	2.496846405	0.952869	0.3520	significant
BB	3.904166667	2.496846405	1.564	0.1336	significant
CC	2.866666667	2.496846405	1.148	0.2645	significant

Source	DF	Sum of squares	MS	F	p-Value	Significant
Model	9	3779.7	419.96	39.122	0.0000	Significant
R-Square = 97.85%						
R-Square Adj. = 87.65%						
R-Square Pred. = 83.55%						
Adeq. Precision = 35.55						
Error	20	920.75	46.037			
Lack of Fit	3	223.95	74.650	1.821	0.1815	
Pure Error	17	696.80	40.988			
Total (Model + Error)	29	4700.4	162.08			

The influence of the operating factors can be estimated by the value and the sign of the coefficients (Oladipo and Gazi, 2014ab). Hence, the positive coefficient of C(BSA/CS-PVA) confirms the factor has linear effect on drug loading efficiency (DC %) while the negative coefficient of A (time) and B (pH) implies an opposite influence. The coefficients of operating factors B (-9.06) and C (8.46) are higher than

that of factor A (-7.83), indicating the significance of BSA/CS–PVA ratio and pH rather than BSA/CS–PVA ratio and time in the loading experiments. Therefore, it can be concluded that pH plays a major role in the loading process.

As shown in Table 2, the model F -value of 39.122 signifies that the quadratic regression model is significant, and only a 0.01% probability that the model this large could take place due to noise. Also, it is concluded that all the values of “**Prob>F**” less than 0.05 indicate that operating terms are significant (Oladipo and Gazi, 2014ab). The data in Table 2 also shows the “**Lack of Fit F-value**” of 1.82 which indicates that it is not significantly comparative to the **pure error**.

The obtained R^2 for BSA loading efficiency shows that the RSM model can explain 97.85% of the changes in the response. The “**Adeq Precision**” ascertains the signal to noise ratio, and a ratio > 4 is adequate for a successful experiment. A ratio of 35.55 in this study implies less noise compared with the signals generated (Ghasemnejad et al., 2015).

4.6 Drug Release Analysis, Optimization, and Mechanism

Various factors (swelling, solvent type, network porosity, molecular weight and nature of the drug) are known to govern drug release from hydrogel (Wang et al., 2010; Nayak et al., 2013).

4.6.1 BSA Release

In this study, BSA release behavior was investigated in a varied glucose concentration, PBS solutions and different pH of the release medium. As seen in Figure 22, the release of BSA from the CS–PVA gel network is pH dependent. The extent of BSA release in PBS (pH 7.4) was observed to be prolonged and higher than

that in PBS (pH 4.0). This observation agrees with the swelling behavior of CS–PVA hydrogel at pH 7.4 and pH 4.0. The cumulative percentage BSA released from CS–PVA hydrogel in 7 h was $86.45 \pm 1.16\%$ at pH 7.4.

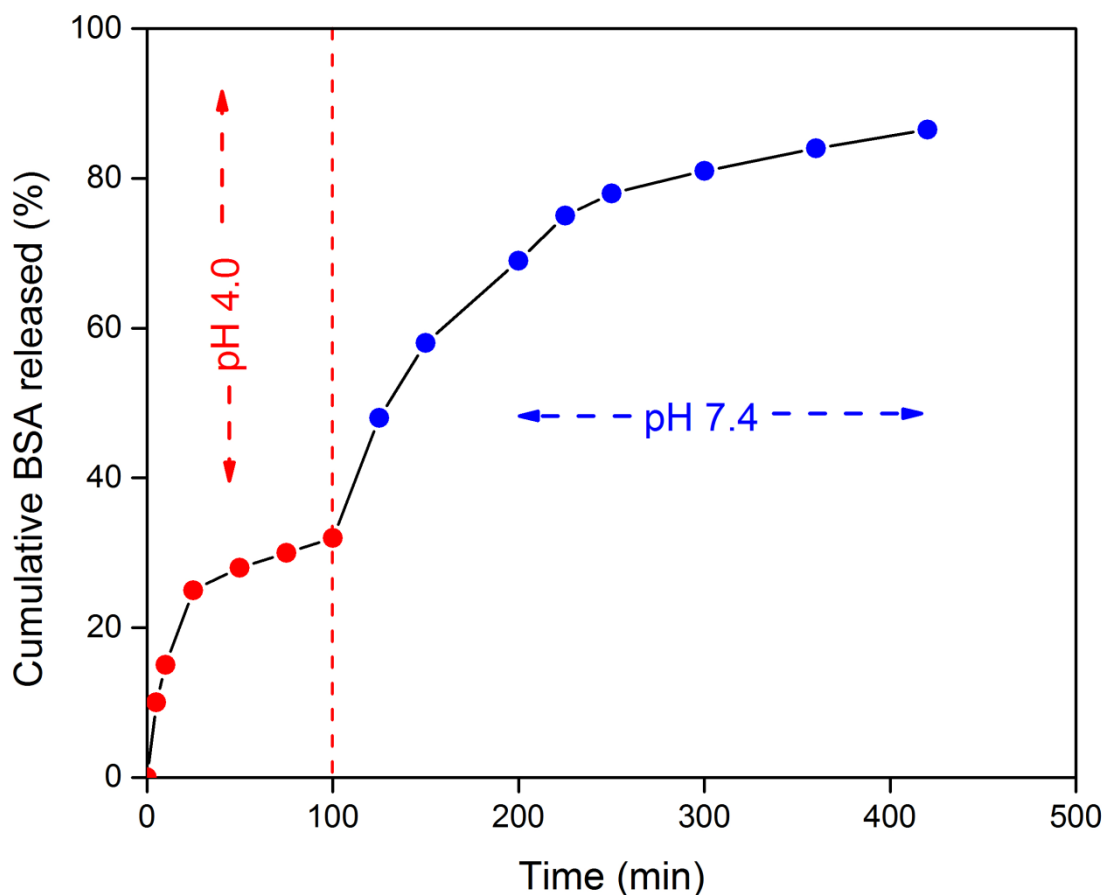


Figure 23. Cumulative release (CR) % of BSA from CS–PVA in different PBS pH

The trace amount of BSA release from CS–PVA hydrogel in the acidic medium could probably be due to the release of surface adhered drug as seen in the SEM image of BSA loaded gel. The cumulative BSA release in response to stepwise changes in glucose concentration (0–5 g/L) was examined to confirm further the glucose-sensitivity of CS–PVA hydrogels system (Figure 23).

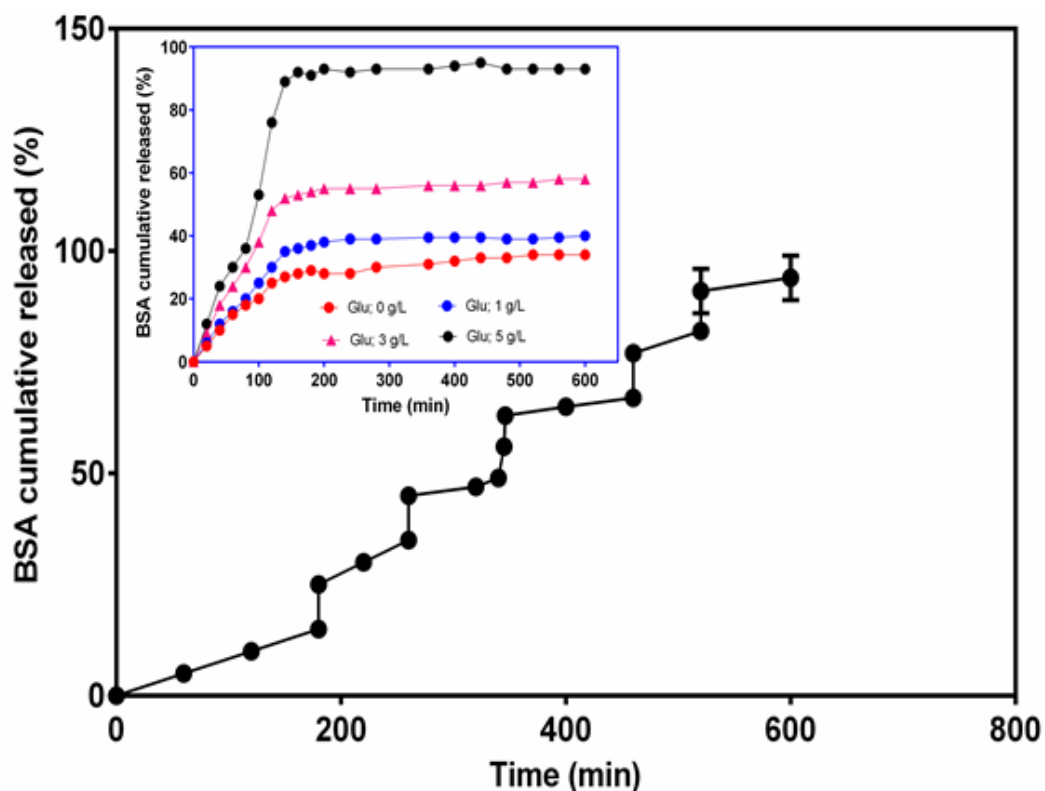


Figure 24. The stepwise response of CS-PVA hydrogels at fixed glucose concentration (5 g/L). BSA cumulative released under different glucose concentrations (insert).

As obtained, the BSA cumulative release amount increased with increasing glucose concentration and had a sudden change at each period. As noted, the BSA release behavior of CS-PVA hydrogels confirmed a glucose concentration-dependent response. Hence, the step-like CS-PVA release behavior for incremental glucose doses evidently proved the versatility of the as-prepared hydrogel to respond to variation in glucose level.

4.6.2 Insulin Release

Here, insulin release behavior was investigated in a varied glucose concentration and PBS solutions in different pH of the release medium. According to Figure 24, the release of insulin from the CS-PVA gel network is pH- and glucose-dependent. In a similar manner like BSA release profile, the extent of insulin release in pH 7.4 was observed to be higher and prolonged than that in pH 4.0. The insulin release profile

from CS–PVA hydrogel reaches the maximum amount of 39–71% in different PBS buffer solutions (in PBS with pH 4.0 after 120 min and in PBS with pH 7.4 after 8 h, respectively).

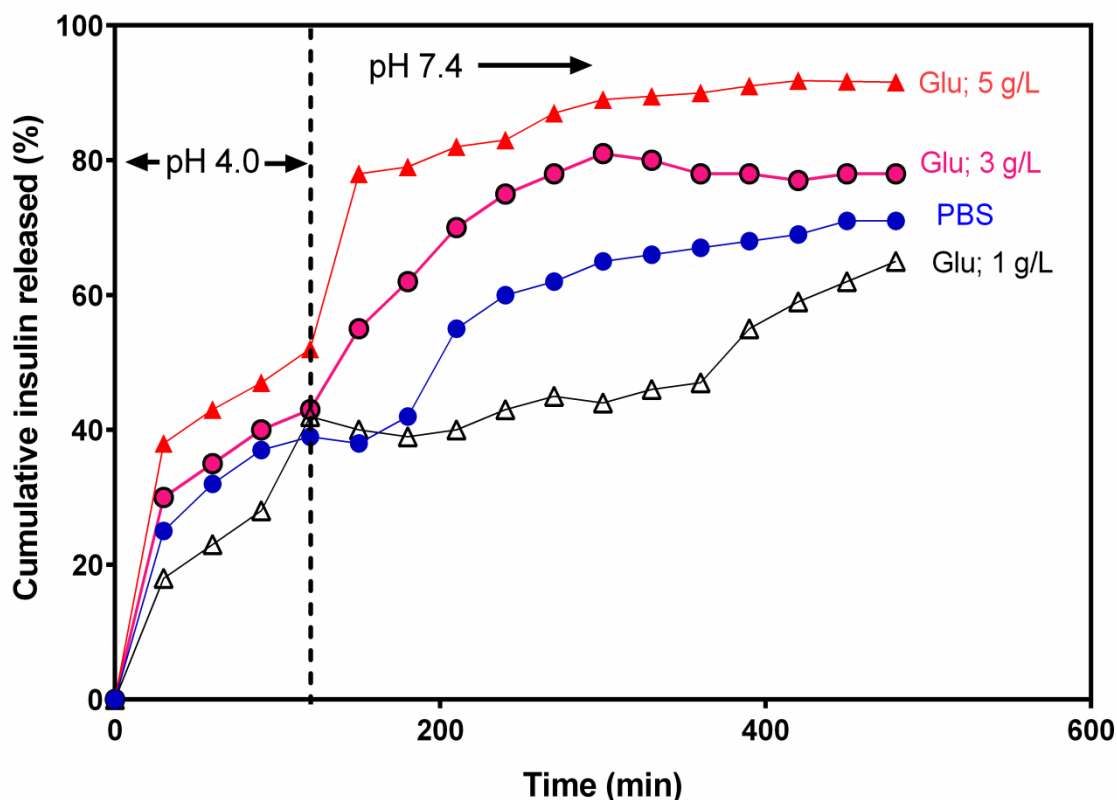


Figure 25. Cumulative release (CR) % of insulin from CS–PVA in different varied glucose concentration and PBS (pH 4 and 7.4)

The cumulative percentage insulin released from CS–PVA hydrogel in the presence of varied glucose concentration (1–5 g/L) after 8 h ranges within 65–92% at pH 7.4. As shown in Figure 24, the amount of insulin released increased with increasing glucose concentration, which confirms the sensitivity of CS–PVA towards glucose.

This observation can be explained by the fact that hydrogen bonding between the CS–PVA and insulin becomes relatively weaker in the presence of glucose, leading to the separation of insulin from the CS–PVA (Ghasemnejad et al., 2015; Mosab et

al., 2015). Also in PBS buffer solution with pH 4.0, the maximum release (39%) occurs within the first 2 h and may be attributed to high concentrations of competing ions.

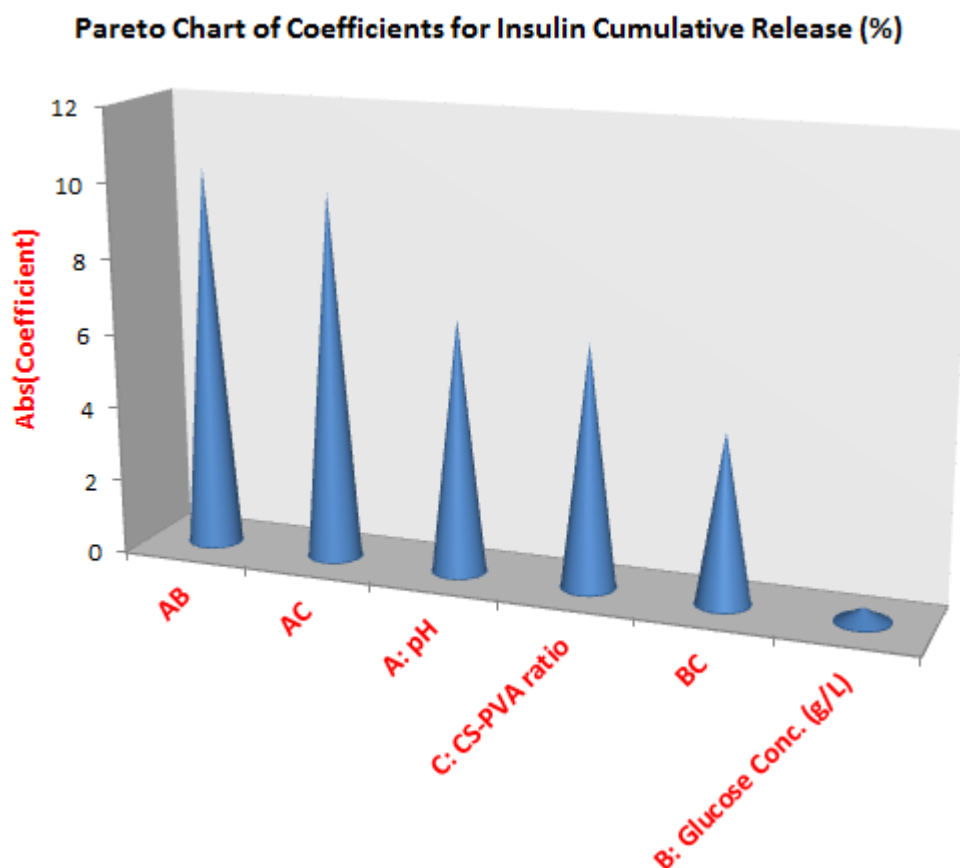


Figure 26. Pareto chart for individual and interactive effects of factors affecting insulin release from CS–PVA hydrogel system

However, the insulin release continues until 8 h in the PBS buffer solution of pH 7.4, and may be due to a lower concentration of competing ions (Wang et al., 2010).

The effects of independent variables (pH, CS–PVA ratio and glucose concentration) upon the dependent variable (cumulative insulin releases) were modeled as shown in Figure 25. The Pareto chart reveals that pH is the most significant factor affecting the insulin release from CS–PVA hydrogel, followed by CS–PVA ratio while the least

factor is glucose concentration. However, the interactive effects of glucose concentration and pH (**AB**) are found to be the most influencing factor.

The observation is consistent with earlier reports on BSA in this study and elsewhere (Zou et al., 2015). In conclusion, the release profile of BSA from CS–PVA hydrogel was affected by three investigated operating factors in the following order; pH > glucose concentration > CS–PVA ratio, while insulin release was influenced in this order pH > CS–PVA ratio > glucose concentration. Also, the release time for BSA/insulin was extended because of the longer path needed for entrapped BSA/insulin to migrate from CS–PVA hydrogel network into the release medium.

4.6.3 Mechanism and Modeling of *In vitro* Release Kinetic of CS–PVA Hydrogel

To investigate and compare the drug (BSA/insulin) release mechanism and profiles, the amount of drug released against time was examined using Higuchi and Korsmeyer–Peppas models respectively (Ghasemnejad et al., 2015; Zou et al., 2015):

$$M_{\text{time}} = k_H \sqrt{t} \quad (6)$$

$$M_{\text{time}} = M_{\infty} kt^n \quad (7)$$

where M_{time} is the total amount of BSA/insulin released after a period t , k_H is the Higuchi constant, $M_{\text{time}}/M_{\infty}$ is the fraction of active BSA/insulin released at time t , n denotes the release exponent (characterize the release mechanism) and k represents the release rate constant.

To investigate release mechanism of BSA and insulin, release, 75% of drug release data were fitted into Higuchi model (Figure 26a-b), and the obtained kinetic parameters are presented in Table 3.

Table 3. Drug release kinetic parameters for CS–PVA in different release media

Drug	Model	R ²	k _H	Release Medium
BSA	Higuchi	0.996	0.0981	PBS (pH 4.0)
		0.987	0.1656	PBS (pH 7.4)
				Glucose Conc.
		0.989	0.1082	0 g/L
		0.995	0.1182	1 g/L
		0.989	0.1398	3 g/L
Insulin	Higuchi	0.992	0.1865	5 g/L
		0.988	0.1563	PBS (pH 4.0)
		0.999	0.1688	PBS (pH 7.4)
				Glucose Conc.
		0.997	0.0982	0 g/L
		0.993	0.1098	1 g/L
	1.000	0.1292	3 g/L	
	0.998	0.1663	5 g/L	

The R² values of the drug release in glucose concentration ranged (0.989–1.000), and that of PBS 4.0 and 7.4 ranged (0.987–0.999). According to the Higuchi model, a linear relationship based on diffusion-controlled mechanism is obtained for the release of drugs uniformly distributed throughout the carrier (Ghasemnejad et al., 2015). Thus, in this study the drug release mechanism from CS–PVA hydrogel was diffusion controlled. Meanwhile, we noticed that the BSA/insulin-loaded on CS–PVA hydrogel in PBS 4.0 and 7.0 displayed a two-step release while those in the presence of glucose showed a one-step release mechanism. Additionally, the k_H values increased with an increase in glucose concentration, indicating that CS–PVA evidently displayed glucose-sensitivity behavior. This observation is consistent with Ghasemnejad et al., (2015) report.

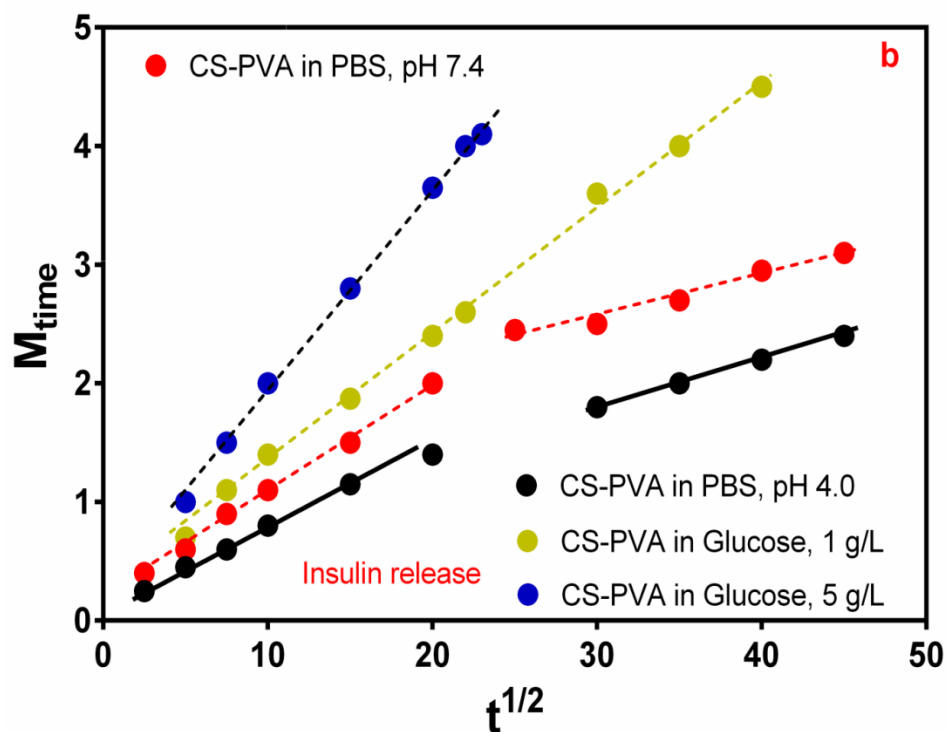
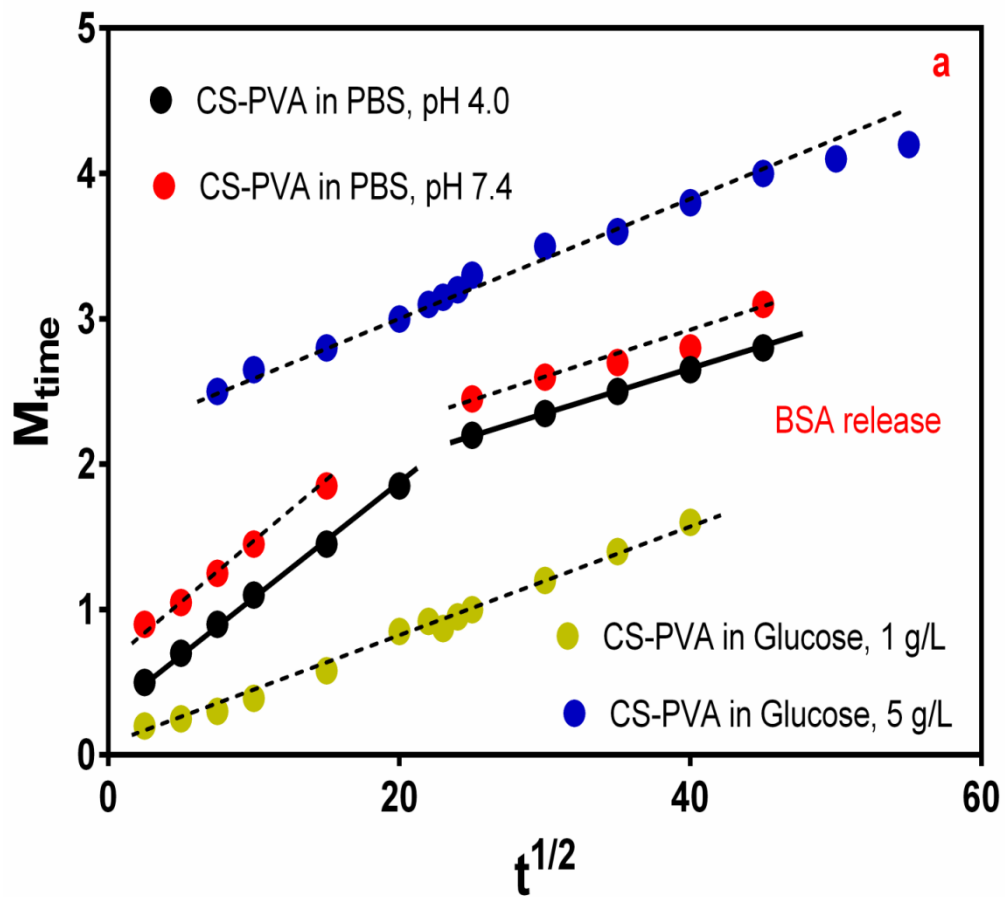
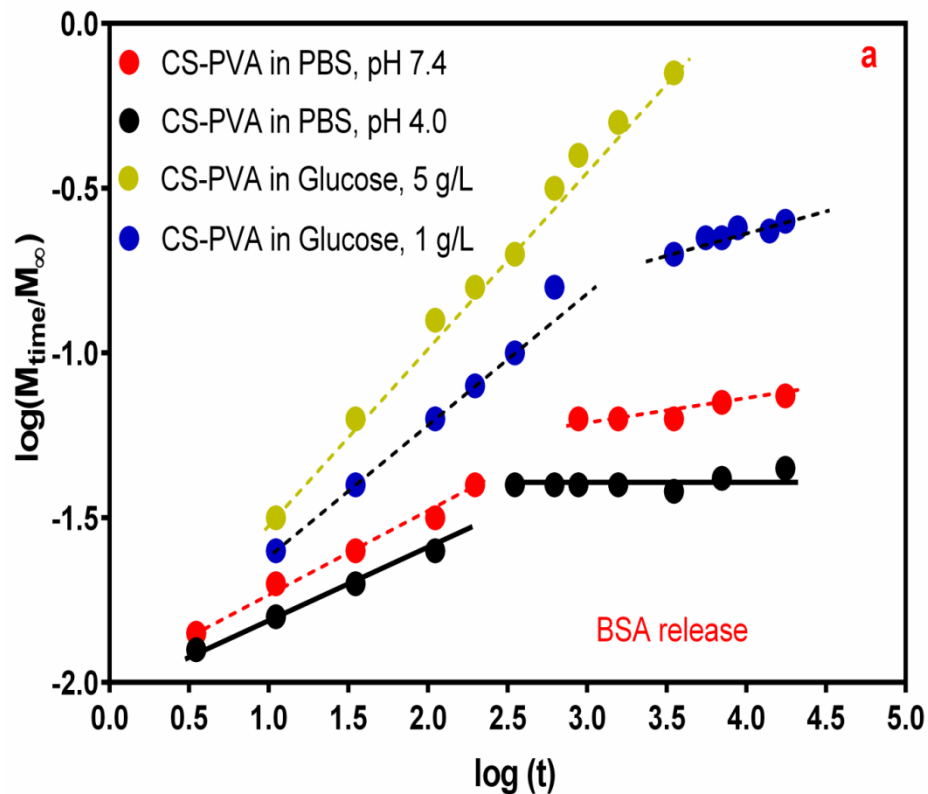


Figure 27. (a) The total amount of BSA and (b) insulin release versus square root of time (Higuchi model)

The experimental data were also fitted to Korsmeyer–Peppas mode. Here, the value of n specifies the drug release mechanism as $0.45 < n < 0.9$ denotes non-Fickian mechanism, $0.45 \leq n$ specifies Fickian transport mechanism, $n > 0.9$ characterize super case II transport mechanism and $n = 0.9$ indicates relaxational case II transport process (Mosab et al., 2015; Zou et al., 2015).

The kinetic parameters obtained by plotting log cumulative percentage of drug release against log time (Figure 27a-b) show that in all glucose concentration, the drug was released by a Fickian diffusion process while those in PBS (4.0 and 7.4) were released by non-Fickian mechanism (Table 4). The Fickian release behavior suggests that diffusion mechanism through the swelling of CS–PVA hydrogel was the major factor in controlling BSA/insulin release.



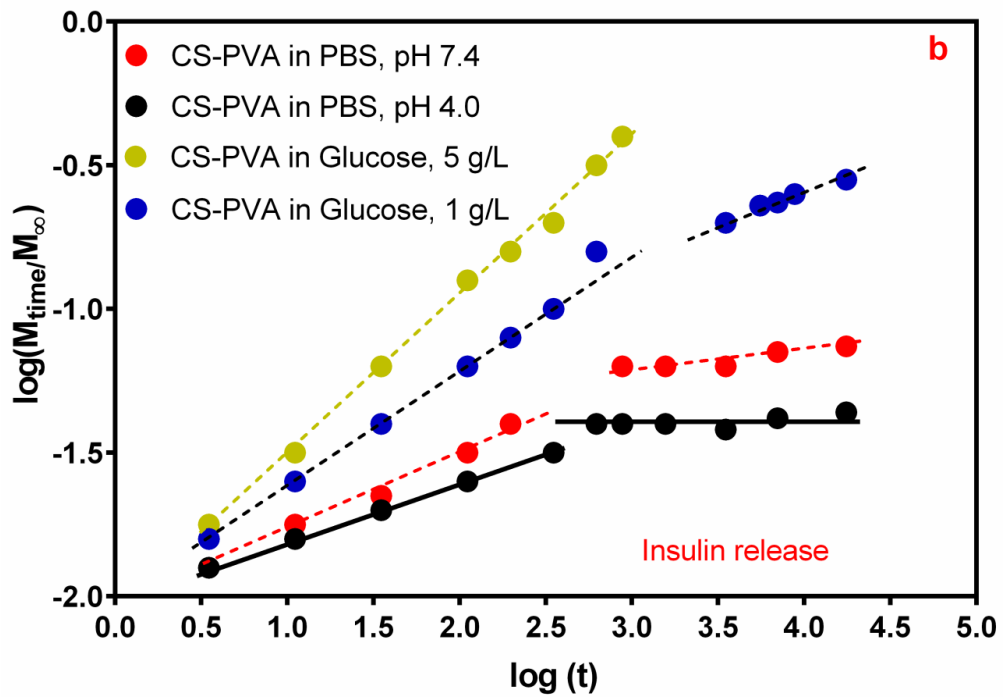


Figure 28. (a) The fraction of BSA released vs. time (b) insulin released vs. time

Table 4. Drug release kinetic parameters for CS–PVA in different release media

Drug	Model	R ²	n	k	Medium	Mechanism
BSA	Korsmeyer–Peppas	0.998	0.5463	0.0237	PBS (pH 4.0)	Non-Fickian
		0.989	0.7345	0.0422	PBS (pH 7.4)	Non-Fickian
					Glucose Conc.	
		0.978	0.3364	0.5298	0 g/L	Fickian
		0.989	0.2353	0.6032	1 g/L	Fickian
		0.999	0.4144	0.6156	3 g/L	Fickian
Insulin	Korsmeyer–Peppas	0.998	0.3199		5 g/L	Fickian
		0.988	0.8051	0.0287	PBS (pH 4.0)	Non-Fickian
		0.997	0.6518	0.0245	PBS (pH 7.4)	Non-Fickian
					Glucose Conc.	
		0.989	0.1358	0.0637	0 g/L	Fickian
		0.999	0.4052	0.0839	1 g/L	Fickian
	0.999	0.1851	0.1235	3 g/L	Fickian	
	1.000	0.1958	0.4833	5 g/L	Fickian	

4.7 Antimicrobial Activity of CS–PVA hydrogel

Minimum inhibitory concentration (MIC) is quite significant to confirm microorganisms' resistance towards antimicrobial agent and to evaluate the activity of the antimicrobial agent. As mentioned earlier, the inhibition zone for gram negative (*E. coli*) bacterial growth using CS–PVA hydrogel was detected visually and shown in Figure 28.

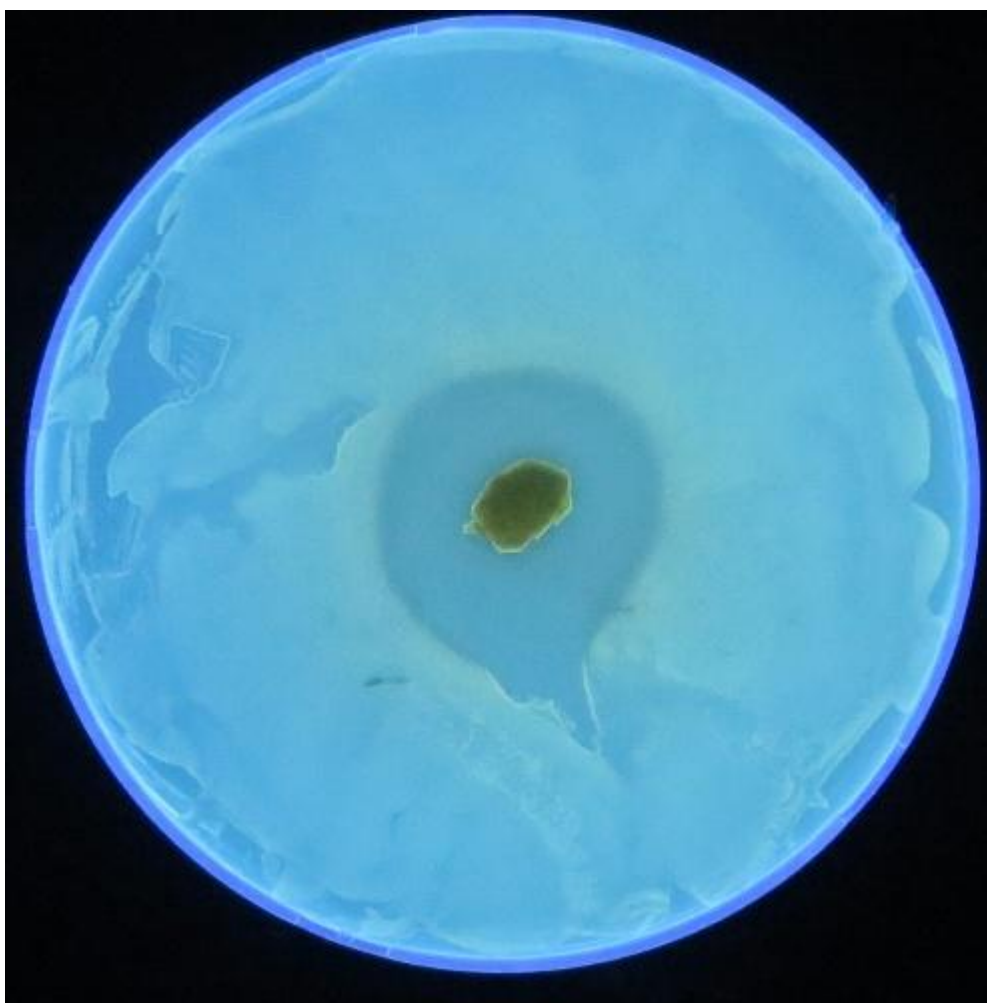


Figure 29. The photograph of the inhibition zones of CS–PVA hydrogel against *E. coli*.

The reduction and inhibition of *E. coli* growth was also determined periodically by measuring the optical density (OD) (viz.; Absorbance at 600 nm) against time and the reduction percentage reported after 24 h as depicted in Figure 29 and 30.

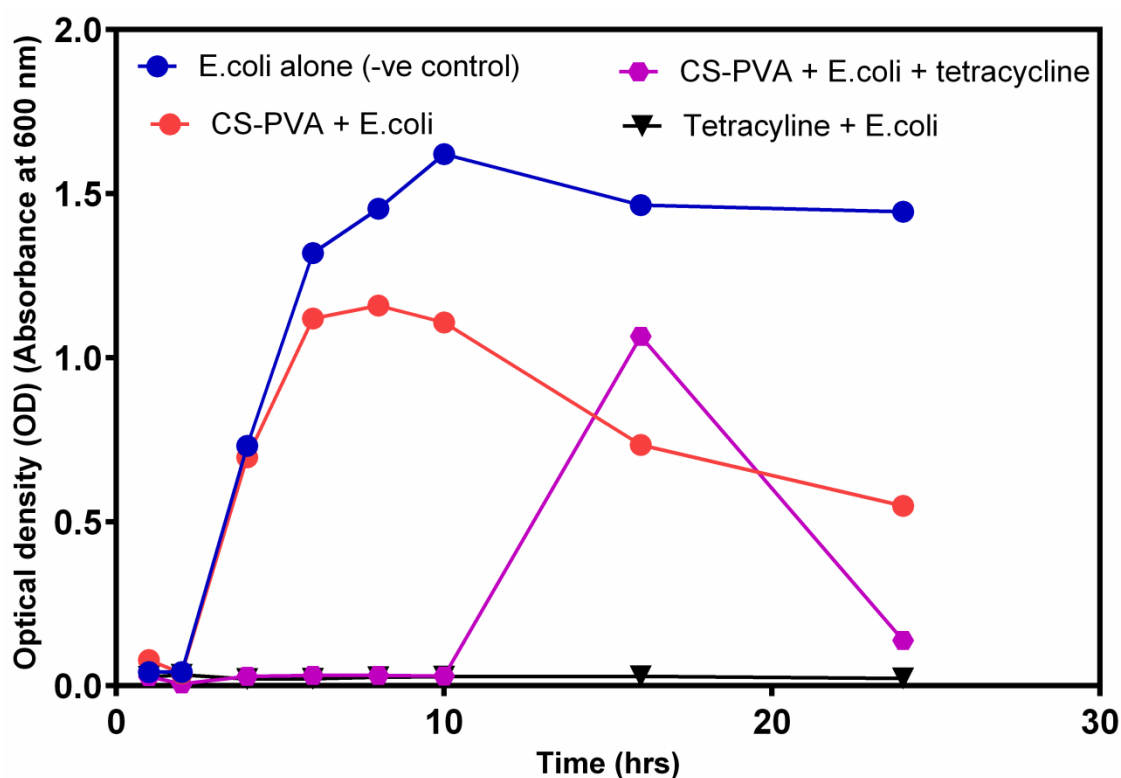


Figure 30. Effect of CS–PVA hydrogel on the growth of *E. coli*

As reported by Benhabiles et al., (2012), the lower the optical density (OD) of the medium, the greater the antibacterial function of the tested material. The CS–PVA hydrogel exhibited inhibitory capability against the *E. coli* growth activity throughout the 24 h incubation period (Figure 29). Meanwhile, the bacteria growth increased rapidly in the control test (-ve) and reached late exponential phase after 10 h with an OD of 1.68.

As shown, the *E. coli* growth was comparably slower in the presence of CS–PVA hydrogels and tetracycline as the late exponential phase was reached after 16 h. The

maximum OD in the experimental group (CS–PVA + tetracycline + *E.coli*) was 1.18; however, 1.25 maximum OD was obtained for the experiment with CS–PVA + *E.coli*. This proves the antibacterial activity of CS–PVA hydrogel and data obtained was consistent with the previous study by Benhabiles et al., (2012).

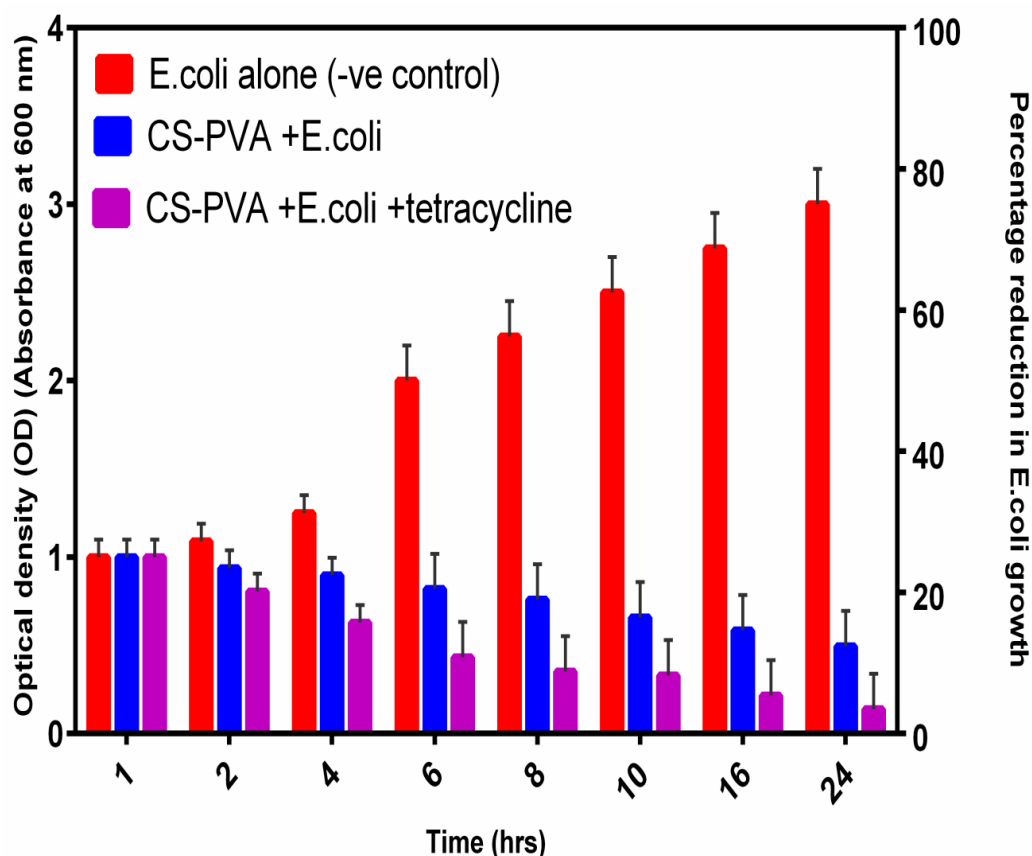


Figure 31. Antibacterial test showing the efficacy of CS–PVA hydrogel against *E.coli*

The antibacterial efficacies of CS–PVA hydrogel and CS–PVA + tetracycline (commercial antibiotic) were evaluated periodically for 24 h against *E.coli* as shown in Fig.30. After 24 h of incubation, there was 86.5% reduction in the growth of *E.coli* for CS–PVA hydrogel and 93% reduction was obtained when tetracycline was introduced. This shows that CS–PVA hydrogel enhanced the antibacterial activity of commercially produced antibiotic (tetracycline).

It can be concluded that the basis for CS–PVA growth inhibition can be attributed to the antimicrobial nature of chitosan coupled with the presence of boric acid that has been utilized for antimicrobial functions. The mechanism of inhibition by the CS–PVA can be explained as thus; the polycationic chitosan interacted with negatively charged components of *E.coli* (gram negative) leading to membrane breakage, loss in *E.coli* cell permeability and possibly death of the bacterial over time.

Chapter 5

CONCLUSION

In the present study, pH- and glucose-responsive hydrogel was prepared from chitosan and poly (vinyl alcohol), and cross-linked with boric acid via cycles of freeze-thawed process.

- The boric acid introduced into the network increased the stability of the hydrogel, can interact with diols (sugars) and enhanced the hydrogel antibacterial activity.
- The experimental results revealed that the synthesized hydrogel swelling and drug release behavior were significantly affected by pH and glucose concentration at physiological conditions.
- The diffusion mechanism of water, acidic and basic solutions into the hydrogel is established to be pseudo-Fickian in nature.
- The optimization results of the drug (BSA/insulin) loading onto CS–PVA hydrogel show that pH and drug/CS–PVA ratios are major factors affecting the loading efficiency.
- The drug release experiments showed the cumulative release of 33.5–86.45% and 39–92% for BSA and insulin respectively at 37 °C in varied glucose concentration and PBS solutions (pH 4.0 and 7.4).
- CS–PVA hydrogel evidently exhibited inhibitory effect against *E.coli* growth.

REFERENCES

- AbdulMujeeb, V.M., Alikutty, P., & Muraleedharan, K. (2014). Synthesis, characterization and vanadium (V) sorption studies on some chitosan derivatives. *Journal of Water Process Engineering*, 143-148.
- Benhabiles, M.S., Salah, R., Lounici, H., Drouiche, N., Goosen, M.F.A., & Mameri, N. (2012). Antibacterial activity of chitin, chitosan and its oligomers prepared from shrimp shell waste. *Food Hydrocolloids*, 48-56.
- Chuang, W., Young, T., Yao, C., & Chiu, W. (1999). Properties of the poly(vinyl alcohol)/chitosan blend and its effect on the culture of fibroblast in vitro. *Biomaterials*, 1479–1487.
- Das, B., Dutta, S., Nayak, A.K., & Nanda, U. (2014). Zinc alginate-carboxymethyl cashew gum microbeads for prolonged drug release: Development and optimization. *International Journal of Biological Macromolecules*, 506-515.
- Evren, M., Acar, I., Guclu, K., & Guclu, G. (2014). Removal of Cu²⁺ and Pb²⁺ ions by N-vinyl 2-pyrrolidone/itaconic acid hydrogels from aqueous solutions. *The Canadian Journal of Chemical Engineering*, 52-59.
- Gade, V.K., Shirale, D.J., Gaikwad, P.D., & Savale, P.A. (2006). Immobilization of GOD on electrochemically synthesized Ppy–PVS composite film by cross-linking via glutaraldehyde for determination of glucose. *Reactive and Functional Polymers*, 1420-1426.

- Gade, V.K., Shirale, D.J., Gaikward, P.D., Savale, P.A., Kakde, K.P., Kharat, H.J., Et, A.I. (2015). Functionalized silica nanoparticles as a carrier for Betamethasone Sodium Phosphate: Drug release study and statistical optimization of drug loading by response surface method. *Materials Science and Engineering C.*, 223-232.
- Islam, A., Riaz, M., & Yasin, T. (2013). Structural and viscoelastic properties of chitosan-based hydrogel and its drug delivery application. *International Journal of Biological Macromolecules*, 119-124.
- Ivanova, A.E., Larsson, H., Galaev, I.Y., & Mattiasson, B. (2004). Synthesis of boronate-containing copolymers of N,N-dimethylacrylamide, their interaction with poly(vinyl alcohol) and rheological behaviour of the gels. *Polymer*, 2495-2505.
- Kim, A., Mujumdar, S.K., & Siegel, R.A. (2014). Swelling Properties of Hydrogels Containing Phenylboronic Acids. *Chemosensors*, 1-12.
- Kim, J., Kim, J., Lee, Y., & Kim, K. (1992). Properties and swelling characteristics of cross-linked poly(vinyl alcohol)/chitosan blend membrane. *Journal of Applied Polymer Science*, 1711–1717.
- Koyano, T., Koshizakib, N., Umeharab, H., Nagurac, M., & Minoura, N. (2000). Surface states of PVA/chitosan blended hydrogels. *Polymer*, 4461–4465.

- Kweon, D. K., & Kang, D.W. (1999). Drug-release behavior of chitosan-g-poly(vinyl alcohol) copolymer matrix. *Journal of Applied Polymer Science*, 458–464.
- Li, Y., Grootendorst, P.V., Rauth, A.M., Abbaspour, M.O., & Abbaspour, M.R. (2015). Optimization of controlled release nanoparticle formulation of verapamil hydrochloride using artificial neural networks with genetic algorithm and response surface methodology. *European Journal of Pharmaceutics and Biopharmaceutics*, 170-179.
- Lin, G. (2010). Development of glucose and ph sensitive hydrogels for microfabricated biomedical sensor arrays. *Ph.DThesis, University of Utah repository*.
- Mahdavinia, G.R., Rahmani, Z., Karami, S., & Pourjavadi, A. (2014). Magnetic pH-sensitive k-carrageenan/sodium alginate hydrogel nanocomposite beads: preparation, swelling behavior and drug delivery. *Journal of Biomaterials Science, Polymer Edition*, 1-16.
- Matricardi, P., Onorati, I., Coviello, T., & Alhaique, F. (2006). Drug delivery matrices based on scleroglucan/alginate/borax gels. *International Journal of Pharmaceutics*, 21-28.
- Mosab, A., Oladipo, A.A., & Gazi, M. (2015). Facile synthesis of glucose-sensitive chitosan-poly (vinyl alcohol) hydrogel: drug release optimization and swelling properties. *International Journal of Biological Macromolecules* .

- Mujtaba, A., Ali, M., & Kohli, K. (2014). Statistical optimization and characterization of pH-independent extended-release drug delivery of cefpodoxime proxetil using Box–Behnken design. *Chemical Engineering Research and Design*, 156-165.
- Nafee, N., Boraie, M., Ismail, F., & Mortada, L. (2003). Design and characterization of mucoadhesive buccal patches containing cetylpyridinium chloride. *Europe PubMed Central*, 199-212.
- Nayak, A.K., Kalia, S., & Hasnain, M.S. (2013). Optimization of aceclofenac-loaded pectinate-poly(vinyl pyrrolidone) beads by response surface methodology. *International Journal of Biological Macromolecules*, 194-202.
- Nayak, A.K., Laha, B., & Sen, K.K. (2011). Development of hydroxyapatite-ciprofloxacin bone-implants using »Quality by design«. *Acta Pharm*, 25-36.
- Nho, Y., & Park, K. (2002). Preparation and properties of PVA/PVP hydrogels containing chitosan by radiation. *Journal of Applied Polymer Science*, 1787–1794.
- Oladipo, A.A., & Gazi, M. (2014). Fixed-bed column sorption of borate onto pomegranate seed powder-PVA beads: a response surface methodology approach. *Toxicological & Environmental Chemistry*, 837-848.

- Oladipo, A.A., & Gazi, M. (2014). Nickel removal from aqueous solutions by alginate-based composite beads: central composite design and artificial neural network modelling. *Journal of Water Process Engineering*.
- Oladipo, A.A., & Gazi, M. (2015). Two-stage batch sorber design and optimization of biosorption conditions by Taguchi methodology for the removal of acid red 25 onto magnetic biomass. *Korean Journal of Chemical Engineering* .
- Oladipo, A.A., & Gazi, M. (2014). Enhanced removal of crystal violet by low cost alginate/acid activated bentonite composite beads: Optimization and modelling using non-linear regression technique. *Journal of Water Process Engineering*, 43-52.
- Oladipo, A.A., Gazi, M., & Saber-Samandari, S. (2014). Adsorption of anthraquinone dye onto eco-friendly semi-IPN biocomposite hydrogel: Equilibrium isotherms, kinetic studies and optimization. *Journal of the Taiwan Institute of Chemical Engineers*, 653-664.
- Oladipo, A.A., Gazi, M., & Yilmaz, E. (2014). Single and binary adsorption of azo and anthraquinone dyes by chitosan-based hydrogel: Selectivity factor and Box-Behnken process design. *Chemical Engineering Research and Design*.
- Panda, S. R., Mukherjee, M., & Sirshendu De. (2015). Preparation, characterization and humic acid removal capacity of chitosan coated iron-oxide-polyacrylonitrile mixed matrix membrane. *Journal of Water Process Engineering* , 93-104.

- Peppas, N.A. (2004). Is there a future in glucose-sensitive, responsive insulin delivery systems? *Journal of Drug Delivery Science and Technology*, 247-256.
- Reddy, R. M., Srivastava, A., & Kumar, A. (2013). Monosaccharide-Responsive Phenylboronate-Polyol Cell Scaffolds for Cell Sheet and Tissue Engineering Applications. *Plos One*, 1-13.
- Sajeev, U., Anoop Anand, K., Menon, D., & Nair, S. (2008). Control of nanostructures in PVA, PVA/chitosan blends and PCL through electrospinning. *Bulletin of Materials Science*, 343-351.
- Uslu, I., Çelikkan, H., Atakol, O., & Aksu, ML. (2008). Preparation of PVA/Chitosan Doped with Boron Composite Fibers and Their Characterization. *Hacettepe Journal of Biology and Chemistry*, 117-122.
- Wang, X., Deng, W., Xie, Y., & Wang, C. (2013). Selective removal of mercury ions using a chitosan–poly(vinyl alcohol) hydrogel adsorbent with three-dimensional network structure. *Chemical Engineering Journal*, 232-242.
- Wilson, G.S., & Hu, Y. (2000). Enzyme-based biosensors for in vivo measurements. *Chemical Reviews*, 2693-2704.
- Yanga, X., Liu , Q., Chen, X., Yua , F., & Zhu, Z. (2008). Investigation of PVA/ws-chitosan hydrogels prepared by combined γ -irradiation and freeze-thawing. *Carbohydrate Polymers*, 401–408.

Zhang, R., Tang, M., Bowyer, A., Eisenthal, R., & Hubble, J. (2006). Synthesis and characterization of a D-glucose sensitive hydrogel based on CM-dextran and concanavalin A. *Reactive and Functional Polymers*, 757-767.

Zhao, L., Mitomo, H., Zhai, M., Yoshii, F., Nagasawa, N., & Kume, T. (2003). Synthesis of antibacterial PVA/CM-chitosan blend hydrogels with electron beam irradiation. *Carbohydrate Polymers*, 439-446.

Zou, X., Zhao, X., & Ye, L. (2015). Synthesis of cationic chitosan hydrogel and its controlled glucose-responsive drug release behavior. *Chemical Engineering Journal*, 92-100.